New PNHN Pincer-Type Ligands and Their Complexes for Transfer Hydrogenation

by

Brandon Konrad

A thesis

presented to the University of Waterloo

in fulfillment of the

thesis requirement for the degree of

Master of Science

in

Chemistry

Waterloo, Ontario, Canada, 2009

AUTHOR'S DECLARATION

I hereby declare that I am the sole author of this thesis. This is a true copy of the thesis, including any required final revisions, as accepted by my examiners.

I understand that my thesis may be made electronically available to the public.

ABSTRACT

The ligand $^tBu_2PC_2H_4NHCH_2Py$ (PNHN) was synthesized starting from 2-pyridinecarboxaldehyde and 2-chloroethanamine. Initial attempts for coordination of the PNHN ligand to a metal center was performed using $[IrCl(COE)_2]_2$, $IrCl_3 \cdot 3H_2O$, $[RuCl_2(p\text{-cymene})]_2$ and $RuCl_2(PPh_3)_3$. The reaction between the PNHN ligand and $[IrCl(COE)_2]_2$ under H_2 resulted in the chloride $IrCl(H)_2(PNHN)$. Synthesis of the active hydride species is currently under investigation. A reaction of the PNHN ligand with $RuCl_2(PPh_3)_3$ under nitrogen afforded the dichloride $RuCl_2(PPh_3)(PNHN)$. Treatment of the dichloride with $KOBu^t$ in 2-pentanol led to the formation of the dihydride $RuH_2(PPh_3)(PNHN)$. Formation of the 16-electron amido complex $RuH(PPh_3)_3(PNN)$ was achieved through the evolution of H_2. The dihydride demonstrated good potential catalytic activity for transfer hydrogenation of acetophenone and cyclohexanone. Current work involves the synthesis of a chiral analogue of the PNHN ligand.

ACKNOWLEDGEMENTS

I would like to thank Professor Dmitry Gusev for giving me the opportunity to achieve a Masters Degree in the field I so dearly enjoy. With his guidance, support and encouragement over the past couple of years, he has given me the necessary tools to succeed in my future endeavours as a chemist. The time I spent under his supervision and in his laboratory was a rewarding experience. A special thanks is extended to Professor Mike Chong who out of his own good nature took the time to help me enrol as a masters student at the University of Waterloo while being able to complete my research at Wilfrid Laurier University. Thanks is also given to Professor Eric Fillion and Mike Chong for taking the time out of their busy lives to be on my committee. Finally I would like to thank Telly for all his help and the many coffee breaks throughout the years; you definitely made things less stressful on numerous occasions.

On a more personal note, I graciously thank my wife Gosia who had the patience and provided the never ending support I needed through the good and bad. I really do not know what I would have done without you by my side. Thanks to my parents for showing their love and believing in me when times got tough. To my brother Nathan who just seemed to know when I needed someone to talk to. And finally to everyone else who always made time to be there when I needed it most and for trying to understand my chemistry, I thank you.

This thesis is dedicated to my wife Gosia

who has given me the strength and confidence to do anything

through her love and understanding.

TABLE OF CONTENTS

LIST OF FIGURES

Chapter One

Chapter Three

Chapter Four

LIST OF TABLES

Chapter Four

LIST OF ABBREVIATIONS

atm	Atmosphere
BINAP	2,2'-bis(diphenylphosphino)-1,1'-binaphthyl
Bu_4NBH_4	*tetra*-butylammonium borohydride
DFT	Density functional theory
DIBAL-H	Diisobutylaluminum hydride
DMF	*N,N*-dimethylformamide
ee	Enantiomeric excess
e^-	Electron
FDA	Food and Drug Administration
h	Hour
Hz	Hertz
IR	Infrared spectroscopy
kcal/mol	Kilocalorie/mole
$KOBu^t$	Potassium *tert*-butoxide
$LiPBu^t_2$	Lithium di-*tert*-butylphosphide
M	molar
min	minute
NaO*i*Pr	Sodium isopropylate
NEt_3	Triethylamine
NMR	Nuclear magnetic resonance
NOE	Nuclear Overhauser effect
N_2	Nitrogen

N. R.	No reaction
OH	Hydroxide
Pd/c	Palladium on carbon
PPh$_3$	Triphenylphosphine
psi	Pound per square inch
Pt/c	Platinum on carbon
Py	Pyridine
R$_s$	Small R-group
R$_b$	Bulky R-group
rt.	Room temperature
s/c	Substrate to catalyst ratio
t	time
TBAF	*tetra*-butylammonium fluoride
TMSCl	Trimethylchlorosilane
TOF	Turnover frequency
THF	Tetrahydrofuran

Abbreviations for multiplicities of ^{1}H NMR, ^{13}C NMR, ^{31}P NMR and IR signals

d	Doublet
dd	Doublet of doublets
dt	Doublet of triplets
m	Multiplet
ppm	Parts per million
s	Singlet
t	Triplet

Chapter 1

1.1 Introduction and Literature Review

The development of new more efficient catalysts for the stereoselective reduction of carbonyl compounds represents a current subject of industrial and academic research. A wide range of transition-metal complexes have been shown to catalyze hydrogenation of ketones. There are two principal ways of adding H_2 across a C=O bond: *via* direct H_2-hydrogenation or transfer hydrogenation. Direct hydrogenation is performed in reaction vessels pressurized with hydrogen gas. Catalytic transfer hydrogenation, using 2-propanol or formic acid as hydrogen donors, allows for new and powerful strategies due to the broad applicability and the ease of performance. Chiral catalysts can be used for asymmetric hydrogenation to produce enantiomerically enriched secondary alcohols. To date homogeneous Ru, Ir, and Rh catalysts have been successfully employed for both transfer hydrogenation and asymmetric hydrogenation.[1,2] One of the earliest catalytic methods for the reduction of ketones was reported by Meerwein-Ponndorf-Verley (Scheme 1.1). In this reaction, a ketone is reduced by isopropanol in the presence of an aluminum alkoxide.[3,4,5]

Scheme 1.1
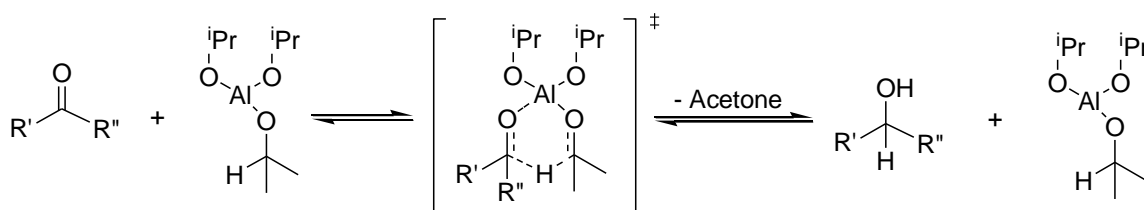
More recent contributions towards the development of new catalysts for transfer hydrogenation were reported by Noyori and co-workers. The catalytic hydrogenation

processes developed by Noyori and co-workers are very attractive. The precatalysts consist of well defined air stable $RuCl_2(PR_3)_2(diamine)$ and $RuCl_2(diphosphine)(diamine)$ complexes used for the generation of active species for homogeneous transfer and asymmetric hydrogenation of ketones[6] and imines[7] in the presence of a base and hydrogen gas.

To date, catalytic hydrogenation of ketones is an important fundamental and indispensable process for the production of a wide range of alcohols and chiral alcohols. These alcohols are valuable end products and precursors for pharmaceutical, agrochemical, flavour, fragrance, material, and fine chemical industries. The pharmaceutical industry uses asymmetric hydrogenation for the synthesis of new organic chemicals, with little to no by-products or wastes. Recent reports have shown that trends in the FDA approval of new drug applications shows the percentage of chiral drugs has increased from 58 % in 1992 to 75 % in 2006.[8] This is because enantiomers of chiral drugs often have dramatically different activities. Atrovastatin (Scheme 1.2, **eq. 1.1**), Rozerem, Enalapril (Scheme 1.2, **eq. 1.2**), and Aliskiren all have been synthesized employing asymmetric hydrogenation.[8]

Scheme 1.2
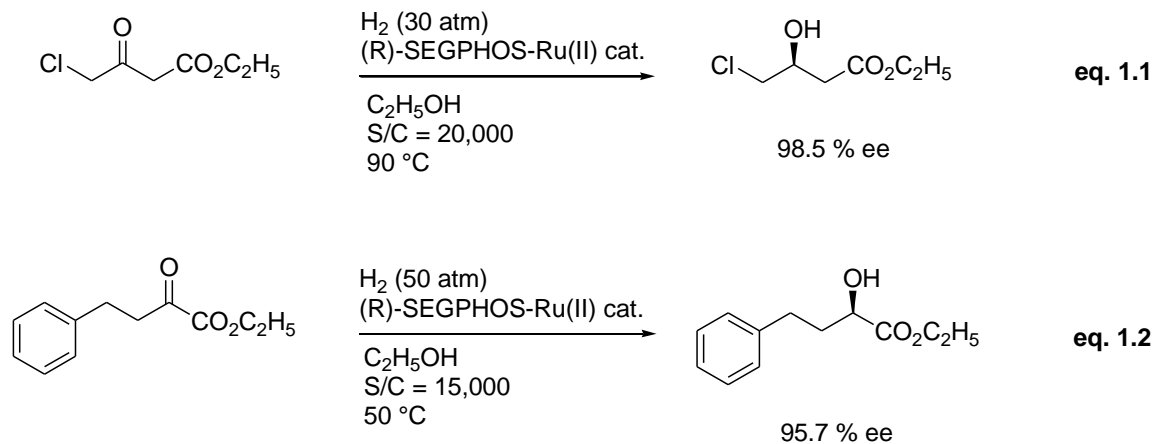
Homogeneously catalyzed ketone hydrogenation has been shown to follow two mechanistic pathways. The bifunctional "outer-sphere" mechanism demonstrates hydrogenation through the simultaneous transfer of the hydridic M-H and protic N-H hydrogens to a C=O bond via a six-atom cyclic transition structure (Figure 1.1, **I**).[9] Alternatively the inner-sphere mechanism takes advantage of an open coordination site on the metal that allows for coordination of an unsaturated substrate followed by insertion into the M-H bond (Figure 1.1, **II**).[9] Both mechanistic pathways may require the presence of a base for catalytic activation generating the catalytically active species. Several groups have recently contributed to a better understanding of the hydrogenation mechanisms both experimentally and computationally.
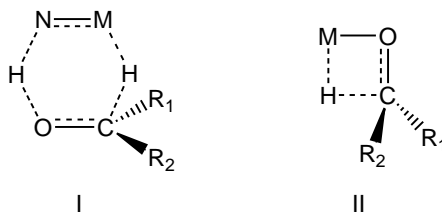
Figure 1.1. Proposed transition states of the bifunctional (**I**) and inner-sphere (**II**) mechanisms.

The objective of this research is to prepare new ligands for use in catalytic hydrogenation through organometallic chemistry. The goal is to synthesize a family of new PNHN pincer-type ligands and their complexes for transfer hydrogenation of ketones and production of secondary alcohols.

1.2 Brief History of Transfer Hydrogenation

In 1968, Knowles and Horner reported the use of a chiral version of Wilkinson's catalyst RhCl(PPh$_3$)$_3$ for homogeneous hydrogenation.[10] Since that discovery, much attention has been given to the design of transition metal hydrogenation catalysts to attain highly efficient molecular transformations for organic synthesis. The bridged hydroxycyclopentadienyl ruthenium hydride (Scheme 1.3, **1**) was reported by Shvo in 1986, and was the first successful example of a bifunctional catalyst.[11] The active catalyst is formed through a reaction with H$_2$ (Scheme 1.3). Under H$_2$, the dimer is cleaved affording RuH(CO)$_2$(C$_5$(OH)Ph$_4$) possessing the required hydridic Ru-H and acidic OH groups.[11]

Scheme 1.3.
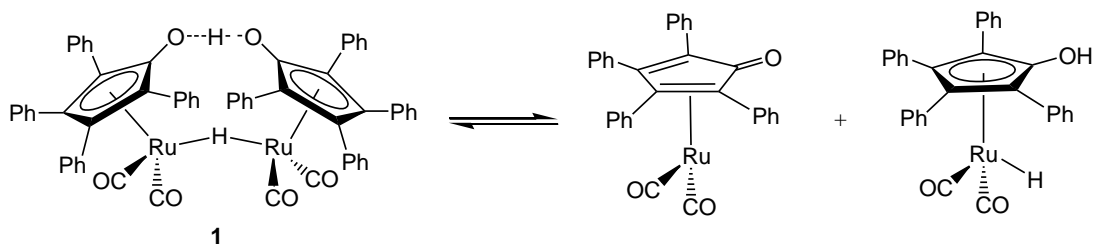
A fundamental contribution to the development of new metal catalysts for transfer hydrogenation and asymmetric hydrogenation has been reported by Noyori and co-workers. Noyori observed that the activity of various ruthenium complexes can be enhanced by using primary amine ligands. Two important catalysts (**2**, **3**) reported by Noyori are shown in Figure 1.2. In the early 1990's, Noyori and co-workers developed Ru-BINAP complexes which could catalyze both transfer hydrogenation and asymmetric hydrogenation. Through manipulation of the accompanying ligand, Noyori reported ruthenium catalysts achieving high TOF and ee values.

2   **3**
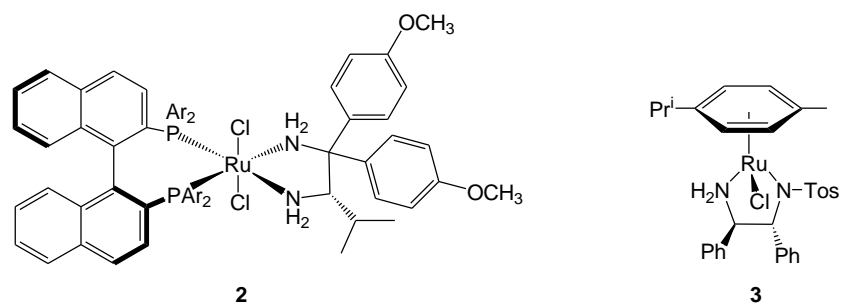
Figure 1.2.

Variations of the Ru-BINAP complexes are used to synthesize chiral secondary alcohols used in the pharmaceutical industry (Scheme 1.4). Recently Noyori and co-workers also demonstrated that chiral η^6-arene-Ru complexes resulted in highly efficient asymmetric hydrogenation of ketones.[9]

Scheme 1.4.

Carbapenems
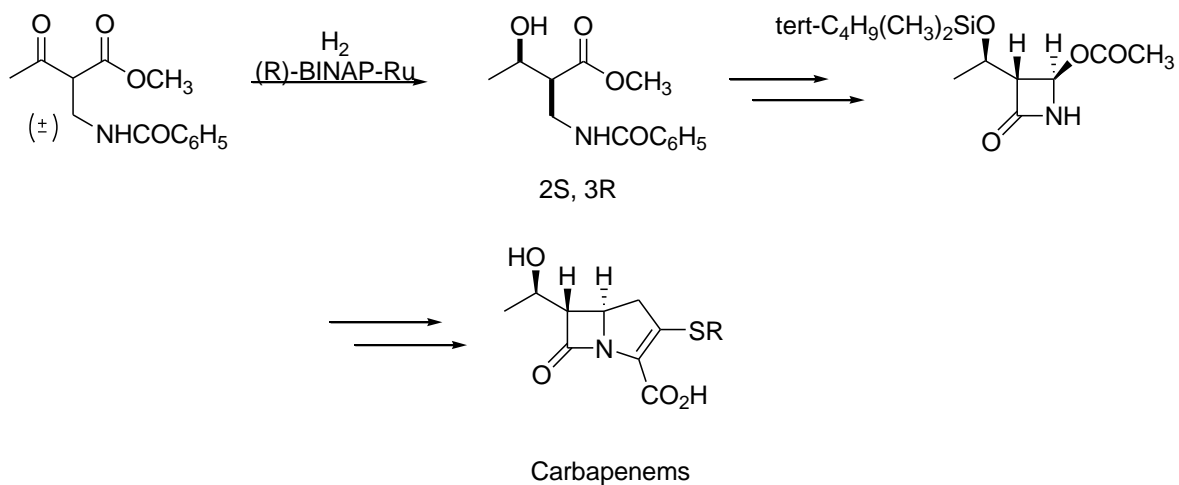
(R)-BINAP-Ru:
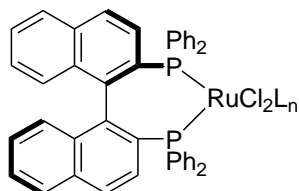
Noyori observed that the activity of ruthenium complexes can be enhanced by the presence of mutually *cis* N-H and Ru-H ligands.[12, 13] For their work in transfer

hydrogenation both Knowles and Noyori received the Chemistry Nobel Prize in 2001 shared with Sharpless.[8]

Another approach for explaining catalytic transfer hydrogenation is with the inner-sphere mechanism. Mizushima and co-workers, Bäckvall, and more recently Stradiotto have demonstrated that ketone hydrogenation can be catalyzed by complexes possessing no protic NH or OH groups. Mizushima and co-workers showed that *cis*-$Ru(H)_2(PPh_3)_4$ is an active transfer hydrogenation catalyst (Scheme 1.5, **eq. 1.3**).[14] It is reasonable to assume that at least one PPh_3 dissociates during the catalytic reaction, opening up a coordination site. Lin and Zhou reported that a variation of Mizushima's catalyst follows the same mechanism and shows higher catalytic activity at room temperature. By replacing one of the PPh_3 groups with an H_2 molecule, the new complex $Ru(H)_2(H_2)(PPh_3)_3$ (Scheme 1.5, **eq. 1.4**) showed an improvement in catalytic activity for transfer hydrogenation.[15] The active catalyst $Ru(H)_2(PPh_3)_3$ is generated through loss of H_2 from $Ru(H)_2(H_2)(PPh_3)_3$.[15] Pàmies and Bäckvall proposed an alternative approach involving $RuCl_2(PPh_3)_3$ as the precatalyst.[16] The active catalyst $Ru(H)_2(PPh_3)_3$ (Scheme 1.5, **eq. 1.5**) is formed through the reaction of $RuCl_2(PPh_3)_3$ with a KOH and 2-propanol.[16] Loss of one of the PPh_3 groups opens a coordination site on Ru where the substrate ketone can coordinate to Ru.

Scheme 1.5.

eq. 1.3

eq. 1.4

eq. 1.5
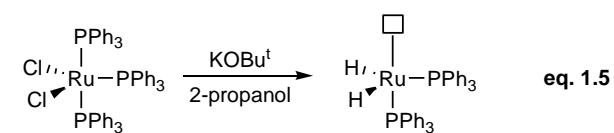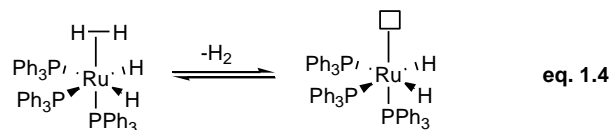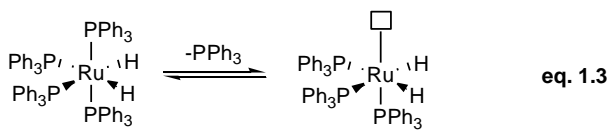
Beyond these examples, Stradiotto has recently developed a catalyst that demonstrates inner-sphere catalysis and also resembles the η^6-arene-Ru catalyst reported by Noyori (Figure 1.3, **3**).[17] Stradiotto's complex (Figure 1.3, **4**) clearly demonstrates that efficient transfer hydrogenation can occur without a protic group on the metal. This is achieved through dissociation of the amine from the metal centre.[17] The resulting open coordination site on Ru is utilized for catalysis.

3

4
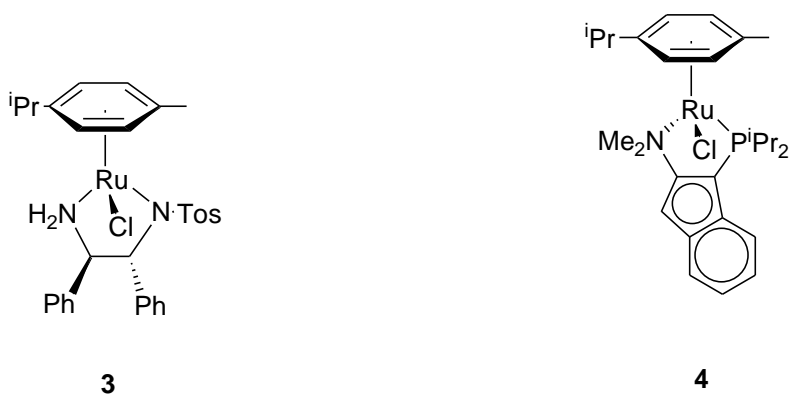
Figure 1.3

1.2.1 Bifunctional Mechanism

Several groups (Noyori, Morris, Casey) have made much progress in developing a good mechanistic understanding of transfer hydrogenation reactions proceeding via the bifunctional mechanism illustrated in Scheme 1.6.

Scheme 1.6

acetone

A

$O=C$ R_1 R_2

N—M
H   H

IV   I

N—M   N—M
D H   H   H   H   B
O—C CH_3 O===C R_1
CH_3 R_2

V H_2

III   II

N===M

2-propanol

C

H
C R_1
HO R_2
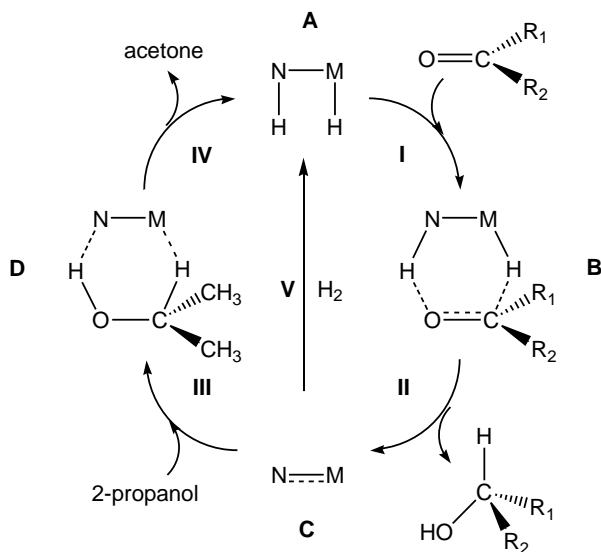
The catalytic cycle in Scheme 1.6 explains the need for the metal hydride M-H and protic N-H group. Through computational and experiment analysis, Noyori has shown the importance of mutually *cis* M-H and N-H groups for bifunctional catalysis. Initially the N-H unit forms a hydrogen bond with the oxygen of the carbonyl.[9] This bond helps bring the carbonyl close to the metal hydride.[9] The ketone substrate then forms a six-membered ring intermediate (**B**) with the metal hydride and protic hydrogen.[18] DFT calculations identify **B** as the transition state in the gas phase. More recent computational work, modeling transfer hydrogenation in solution, suggests that the transition structure **B** would most likely include at least one solvent molecule as shown in Scheme 1.7.[19]

Scheme 1.7
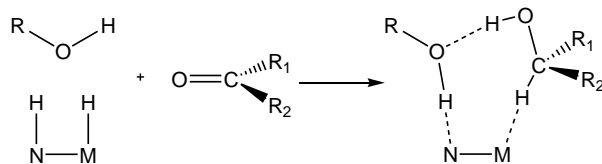
Step **II** completes the transfer of the hydride and protic hydrogens to the C=O, forming a secondary alcohol and a 16-electron amido metal complex (**C**). The amido complex is stabilized by a partial double bond between the metal and nitrogen.[9] From this point, two possible paths can be used to regenerate the active catalyst. The first pathway uses H_2 gas to reduce the partial M-N double bond (step **V**). Coordination of H_2, formation of an intermediate dihydrogen complex and subsequent heterolytic cleavage of the H-H bond would regenerate the active catalyst.[20] The heterolytic cleavage of the H_2 molecule can occur through the four-membered intermediate (**5**) or the six-membered intermediate (**6**) mediated by the hydrogen bonded alcohol.
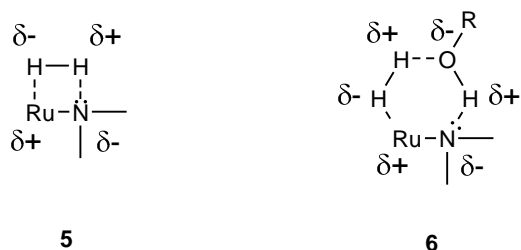
Figure 1.4. Heterolytic cleavage of an H_2 molecule intermediates.

The second pathway (step **III**) uses 2-propanol as the hydrogen source (formic acid can also be used as the hydrogen source). It is proposed that 2-propanol coordinates with the amido complex forming a six-membered ring intermediate. The OH group of 2-propanol forms a hydrogen bond with the amido nitrogen followed by the formation of a C···H···M interaction.[21] This is illustrated by the intermediate structure **D**. Regeneration of the

active catalyst is completed by dissociation (**IV**) of acetone. Specific examples of catalysts that follow the bifunctional mechanism will be discussed later.

1.2.2 Inner-Sphere Mechanism

Well-defined examples of bifunctional catalysts are 18-electron saturated complexes, a distinctive feature of the inner-sphere mechanism is that it requires an unsaturated 14 or 16-electron catalyst.

Scheme 1.8
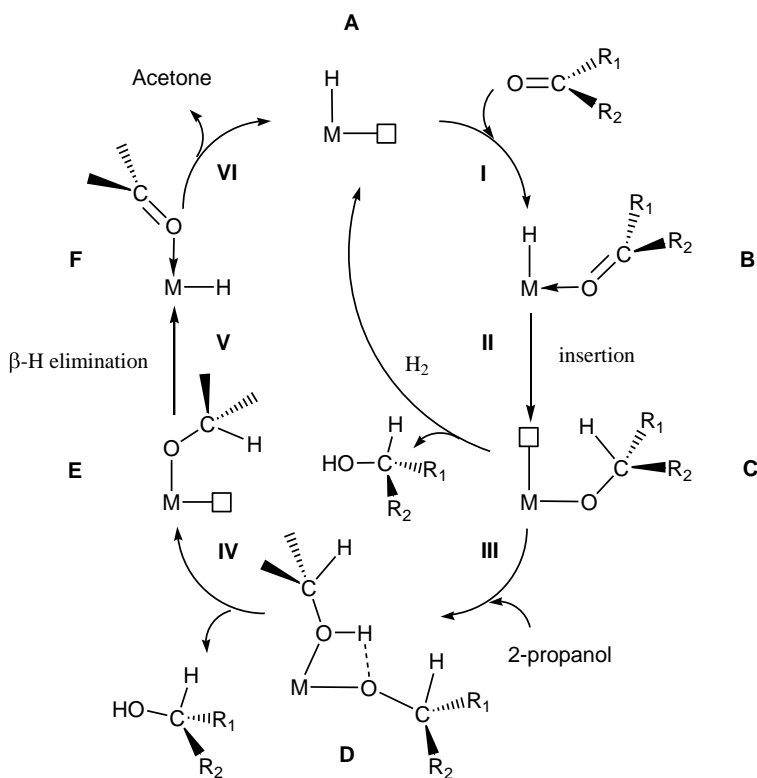
This unsaturated catalyst allows for coordination of the substrate ketone directly to the metal center. The empty coordination site is a result of ligand dissociation from the starting 18-electron metal complex in solution (**A**). Step **I** (Scheme 1.8) shows the ketone coordinating to the unsaturated metal center (**B**). An insertion of the substrate into the M-

H bond affords a new unsaturated metal complex (**C**).[22] At this point the hydrogen source, 2-propanol, can coordinate with the unsaturated metal (step **III**). This coordination is followed by a proton transfer from the OH group of 2-propanol to the oxygen of the substrate (**D**).[22] The result is the release of a secondary alcohol (step **IV**) and a new open coordination site on the metal center (**E**). Step **V** involves a β-H elimination (**F**) resulting in the release of acetone (step **VI**).[22] This final step results in the regeneration of the active catalyst. A second pathway involves the use of H_2 gas as the hydrogen source. Coordination of an H_2 molecule to the metal center (**C**) occurs via an open coordination site. Subsequent heterolytic cleavage of the coordinated H_2 results in the release of a secondary alcohol and regeneration of the active catalyst.[22]

1.2.3 Difficulties Determining Mechanistic Pathways

Though there are many examples of complexes that follow either the bifunctional or inner-sphere mechanisms, determining the correct mechanistic pathway can require extensive experimental and computational analysis. The Shvo catalyst is one of the most paradigmatic hydrogenation catalysts due to its immense versatility. Its applications in transfer hydrogenation include hydrogenation of carbonyls [23], imines [24], alkynes [25], oxidation of alcohols[26] and amines[27] amongst many others. The mechanism of the Shvo catalyst has been one of the most controversial in regards to the nature of the hydrogen transfer. Shvo and coworkers showed that with activation of the catalyst using H_2, transfer hydrogenation occurs through the concerted outer-sphere mechanism (Scheme 1.9, **I**).[23] Regeneration of the active catalyst is achieved through one of two possible pathways. The first being formation of complex **1** (Scheme 1.9) from **II** followed by

11

subsequent activation with H_2.[23] The second pathway involves coordination of one molecule of formic acid (**III**) followed by liberation of CO_2.[23]

Scheme 1.9
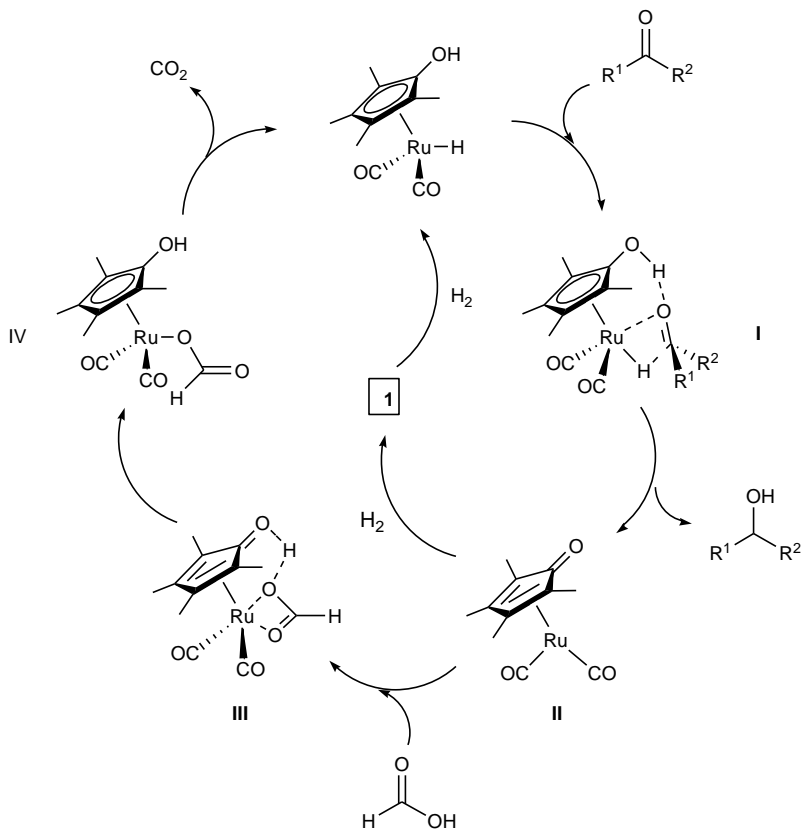
Recently, computational analysis by Casey's and Bäckvall's group has given rise to alternative catalysis mechanisms. In 2001, Casey's group used the tolyl analogue of the Shvo catalyst [2,5-Ph$_2$-3,4-Tol$_2$(η^5-C$_4$OH)]Ru(CO$_2$)H and analyzed the effects of the primary deuterium isotope on the hydrogenation of PhCHO.[28] They concluded that the hydrogenation goes through the concerted bifunctional mechanism. Bäckvall's work supported a concerted mechanism but taking place through an inner-sphere mechanism via a η^5 - η^3 ring slip forming the intermediate **14** as seen in Scheme 1.10.[29]

Scheme 1.10
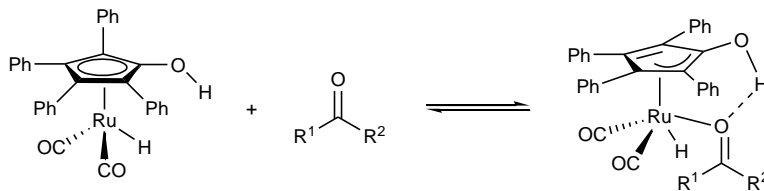
14

Comas-Vives and coworkers investigated both proposed mechanisms with the help of computational analysis. They determined that the concerted inner-sphere H^+ and H^- transfer through the η^5-η^3 ring slippage would have an energy barrier of 34.6 kcal/mol in solution.[28] The investigation of the H^+ and H^- transfer of the bifunctional mechanism resulted in an energy barrier of 7.7 kcal/mol in solution.[28] With these results, it was concluded that the bifunctional mechanism presented the most favourable energy pathway. Through computational and experimental analysis it seems to be clear that the bifunctional mechanism is more feasible.

Beyond the Shvo catalyst, Baratta and coworkers reported the synthesis of complex **15** where the mechanism was reported to follow the inner-sphere transfer.
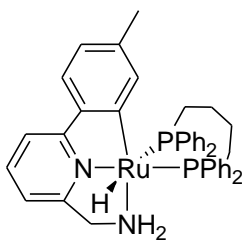
15

Figure 1.5

They reported that with the active catalyst, an NH···O=C interaction results activating the substrate towards nucleophilic attack and provides the ketone with the orientation needed for transfer of the hydride (Scheme 1.11).[30] This resulting alkoxide

anion can then migrate from the hydrogen to the metal center affording the Ru-alkoxide intermediate **16**.[30] The theoretical studies performed by Baratta and coworkers also supported this mechanistic pathway.[30] The reversibility of the alkoxide formation when using benzophenone provides evidence that the Ru-alkoxide is an intermediate in the formation of the hydride.

Scheme 1.11
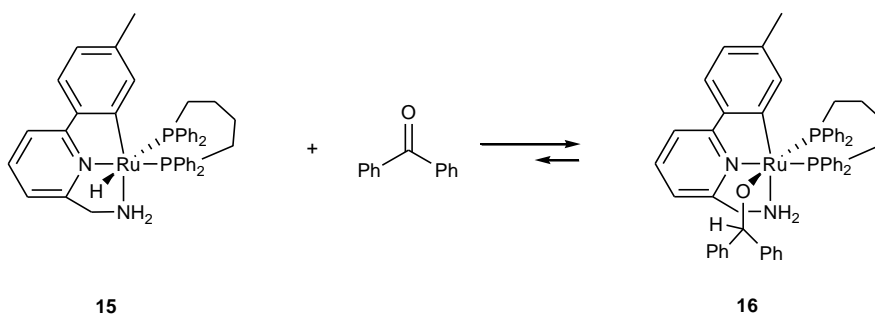
The two aforementioned catalysts illustrate the difficulties that can arise when attempting to determine the correct mechanistic pathway of a reaction.

1.3 Bifunctional Catalysts

Using transition metal catalysts, the kinetics, TOF and ee of reactions following the bifunctional mechanism have been reported extensively. An ideal catalyst should have high TOF's for a wide range of substrates, and the reactions should be easy to perform, safe, and environmentally friendly.[31]

Noyori and Ohkuma disclosed the catalyst **2** as being efficient for asymmetric hydrogenation of a large variety of ketones.[31] In the general reaction (Scheme 1.12) **2** was used to perform asymmetric hydrogenation to demonstrate the catalytic capabilities of the Ru-BINAP complex.[31]

Scheme 1.12
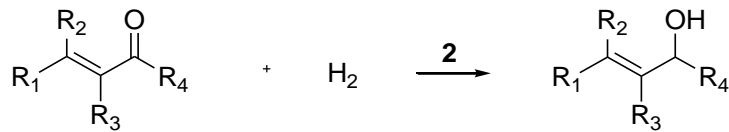
Manipulations to the accompanying ligand allowed them to perform asymmetric hydrogenation on ketones with a range of functional groups including aromatic and alkene groups. These reactions were used to verify the versatility of the Ru-BINAP complex. Figure 1.7 lists some of the results demonstrating high enantioselectivity.

| 99 % ee | 100 % ee | 97 % ee | 94 % ee | 97 % ee |
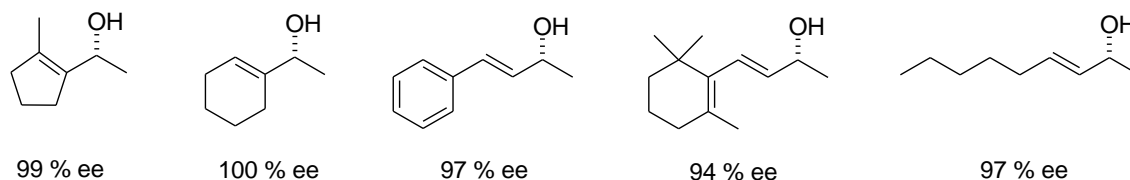
Figure 1.7. Alcohols produced by transfer hydrogenation of ketones using **2**, K_2CO_3 or KOBu^t as the base, 8-10 atm H_2 (S/C = 2000:1 – 13000:1) or 80 atm H_2 (S/C = 100000:1), at 25-30 °C.[31]

Though a major goal is to achieve high enantiomeric selectivity, numerous complexes have been reported showing high TOF. This is important when the aim is to achieve high yields using minimal catalyst loadings. With the pharmaceutical industry emphasis is placed on producing secondary alcohols with high enantiomeric selectivity. Conversely, in an industry where high enantiomeric selectivity is not as vital, high TOF values are more desirable. This is the case with the oil and gas industry where catalysts achieving high TOF numbers are of more interest.

7   **8**
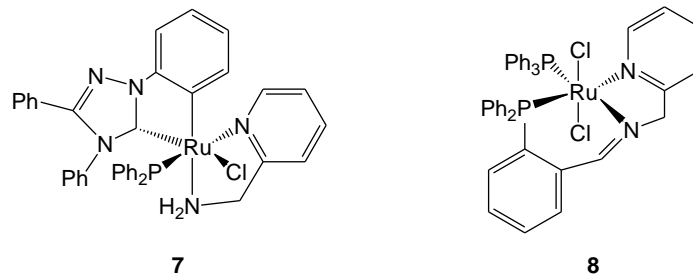
Figure 1.8

Many sophisticated bi-, tri-, and tetradentate achiral and chiral ligands have been successfully used to prepare five- and six-coordinate complexes for transfer hydrogenation. Some of these species include [RuCl$_2$(P)$_2$(NN)] (NN = diamine, dipyridine)[32], [RuCl$_2$(P)(NPN)][33], [RuCl$_2$(NPN)][34] (NPN = oxazoline based ligands), and [RuCl$_2$(PNNP)] (PNNP = diphosphine/diamine ligand).[35] More recently, Baratta reported the synthesis of an *N*-heterocyclic carbene ruthenium catalyst **7** (Figure 1.8). This catalyst showed high activity in a series of transfer hydrogenation reactions with various ketones (Figure 1.9) demonstrating high TOF values.

Yield = 99 % (5)   Yield = 98 % (2)   Yield = 99 % (5)   Yield = 96 % (10)   Yield = 90 % (10)
TOF = 110000 h^{-1} TOF = 120000 h^{-1} TOF = 100000 h^{-1} TOF = 70000 h^{-1} TOF = 50000 h^{-1}
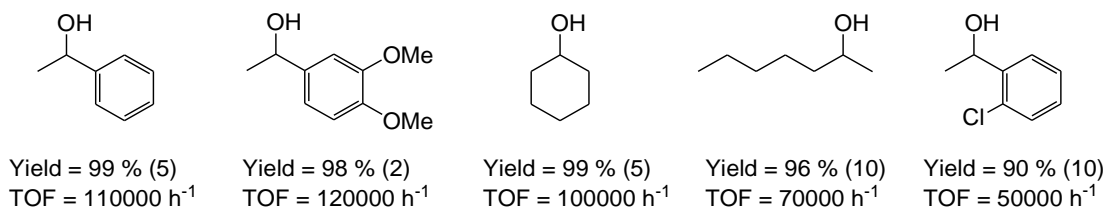
Figure 1.9. Alcohols produced by transfer hydrogenation at 82 °C, 0.1 M of ketone in 2-propanol with NaOH and **7** (2000:1:40).[36]

In 2007, Del Zotto and Baratta reported the synthesis of the complex [RuCl$_2$(PPh$_3$)(PNN')] **8** (Figure 1.8).[37] This complex successfully catalyzed transfer hydrogenation of numerous ketones with a very high rate (TOF up to 250 000 h^{-1}) (Figure 1.10). The high activity of this complex suggests that the imine fragment of the PNN

ligand is probably reduced in the catalytic solution giving the amine NH moiety required for bifunctional catalysis.[37]

Yield = 98 % (2)	Yield = 99 % (1)	Yield = 99 % (1)	Yield = 97 % (5)	Yield = 93 % (10)
TOF = 185000 h^{-1}	TOF = 250000 h^{-1}	TOF = 240000 h^{-1}	TOF = 70000 h^{-1}	TOF = 18000 h^{-1}
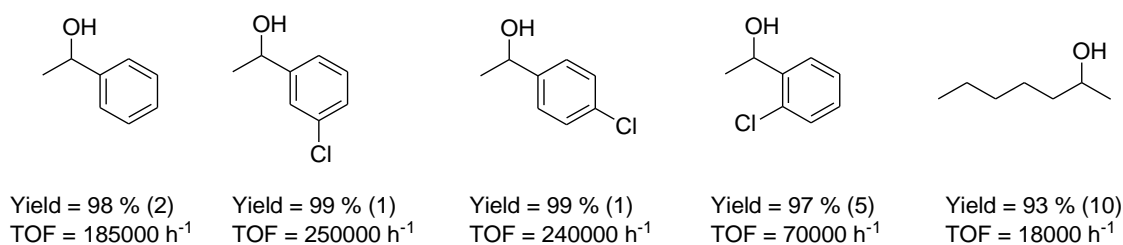
Figure 1.10. Alcohols produced by transfer hydrogenation at 82 $^{\circ}$C, 0.1 M of acetophenone in 2-propanol with (CH$_3$)$_2$CHONa and **8** (1000:1:40).[37]

Del Zotto noted that efficient catalysis with [RuCl$_2$(PPh$_3$)(PNN')] was observed with the presence of the chloride atom in the ortho position resulted in lower TOFs (70 000 h^{-1}). This trend was rationalized to be the result of steric hindrance, which is kinetically relevant when the chloride was located in the ortho position.[37]

Transfer hydrogenation has also been shown to perform in conjunction with other catalytic reactions. Morris developed a Ru-BINAP complex to promote a Michael addition followed by enantioselective transfer hydrogenation according to Scheme 1.12. Motivation for this work came from an earlier report that showed borohydride complexes of the make-up *trans*-RuH(η^1-BH$_4$)(BINAP)(diamine) are active catalysts for asymmetric hydrogenation of ketones without activation using a base.[38] The resulting product alcohol (Scheme 1.12) was obtained as a 30:1 mixture of the *trans* and *cis* isomers; the preferred formation of the *trans* isomer is rationalized through sterics.[38]

Scheme 1.12.[38]
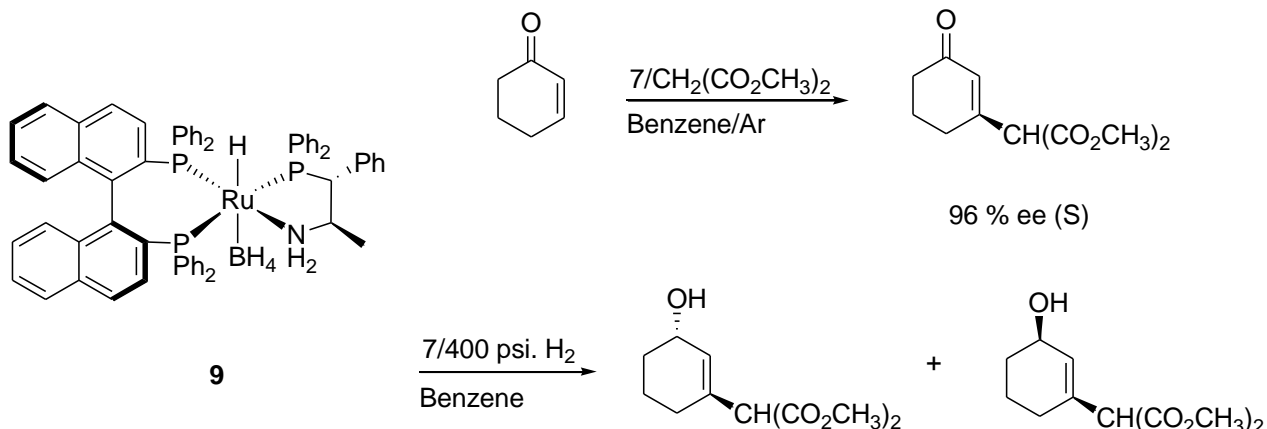
The complexes surveyed in this chapter are just a few of a number of known catalysts that demonstrate good catalytic activity with the NH moiety required by the bifunctional mechanism.

1.4 Inner-Sphere Catalysts

Recently, catalysts have been developed that show comparable TOF values and yields to bifunctional catalysts while following the inner-sphere mechanism. In a report published by van Koten and co-workers in 2007, the synthesis and catalytic activity of the PCP-pincer Ru(II) complex is described (Figure 1.11).[39] The complexes catalytic activity was tested through transfer hydrogenation of cyclohexanone (Figure 1.12). By varying the groups on phosphorus, they noted a change in TOF values ranging from 8 000 to 38 000 h^{-1}.[39]
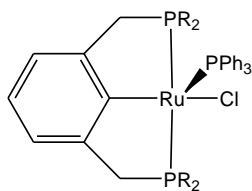
10

Figure 1.11. Ruthenium catalyst **10**, R = $MeOC_6H_4$, $CF_3C_6H_4$, Ph.[39]

| TOF = 33600 h⁻¹ (10) | TOF = 8000 h⁻¹ (30) | TOF = 35700 h⁻¹ (10) |
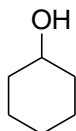
TOF = 33600 h^{-1} (10)   TOF = 8000 h^{-1} (30)   TOF = 35700 h^{-1} (10)
R = Ph   R = $MeOC_6H_4$ R = $CF_3C_6H_4$

Figure 1.12. R represents the groups on phosphorus in **10**. Reactions done at 82 ^{o}C, with 2.0 mmol of cyclohexanone, [Ru] = 0.1 mol%, 2 mL of 2-propanol with NaOH as the base.[39]

  The active catalyst is formed by reacting **10** with NaO*i*Pr in 2-propanol at 82 ^{o}C affording **11**. They determined that the catalytic cycle starts by coordination of the ketone substrate to the Ru-hydride intermediate **12** giving **I** (Scheme 1.13). This coordination is followed by the intermolecular addition of the hydride to the α-C atom of the ketone **II**.[39] 2-propanol releases the coordinated alkoxide through protonation forming the secondary alcohol **III** and **IV**. The catalytic cycle is completed with a hydride transfer from the isopropoxide via β-H elimination (**V**) followed by the exchange of acetone with another substrate molecule ketone resulting in formation of **I**. [39]

Scheme 1.13
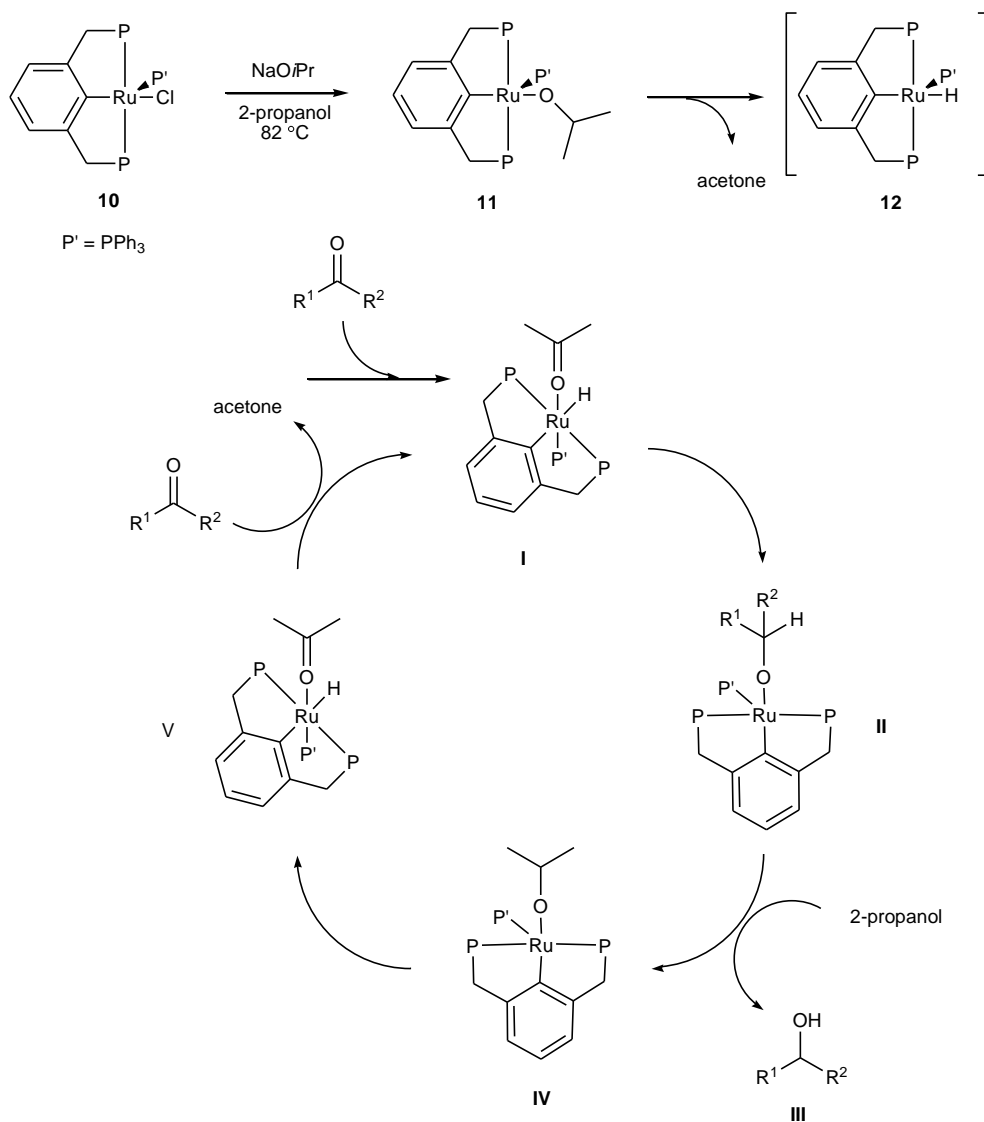
Another interesting example of inner-sphere catalysis was reported by Stradiotto and co-workers. Stradiotto developed a zwitterionic ruthenium complex (Scheme 1.14) that is one of the most active transfer hydrogenation catalysts for ketones to date.[17] When used in reactions with alkyl and aryl ketones, this catalyst demonstrated very high TOF values and near quantitative conversions.[17]

Scheme 1.14

13
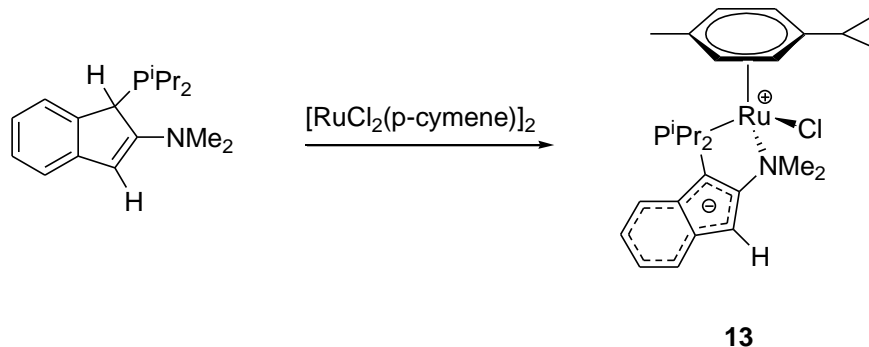
The mechanistic pathway for transfer hydrogenation catalyzed by **13** has been extensively studied by Gusev and Stradiotto with the help of DFT calculations.[40] Activation of the precatalyst (**I**) is achieved with KOBu^t in 2-propanol (Scheme 1.15)[40] resulting in the formation of a 2-propoxide complex (**II**). Dissociation of NMe$_2$ from Ru opens up a coordination site on Ru (**III**). The new 16-electron 2-propoxide intermediate undergoes β-H elimination affording the catalytically active hydride species **IV**.

Scheme 1.15
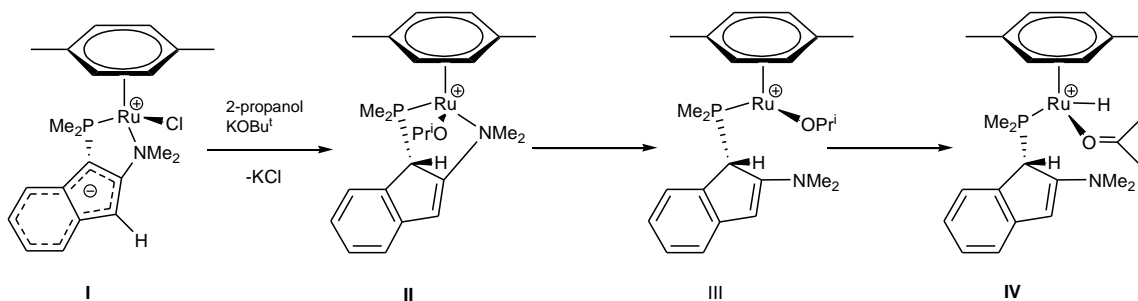
To determine the catalytic activity of **13**, Stradiotto performed transfer hydrogenation using several ketones (Figure 1.13). The resulting TOF values are some of the highest reported.

t(min) = 5
TOF = 180000 h^{-1}

t(min) = 5
TOF = 220000 h^{-1}

t(min) = 15
TOF = 180000 h^{-1}

t(min) = 5
TOF = 180000 h^{-1}

t(min) = 15
TOF = 150000 h^{-1}
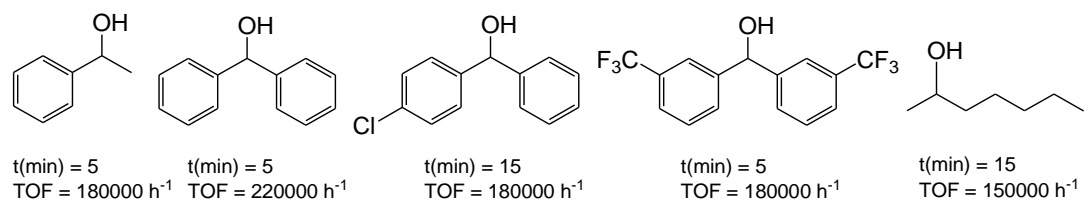
Figure 1.13. Alcohols produced by transfer hydrogenation using of 0.1 M of ketone, **13** at 0.05 mol% in 2-propanol with KOBu^t.[17]

1.6 Research Plan

Based on the literature precedent for the need of a versatile catalyst for transfer hydrogenation, methods to prepare catalysts and analyze their reactivity are proposed. The anticipated strategy for the preparation of transition metal catalysts is to first synthesize a new PNHN pincer-type ligand (Scheme 1.16, **eq. 1.6**). Upon successful synthesis of the proposed PNHN ligand, precatalyst metal complexes will be prepared through coordination with selected transition metals (Ru, Ir, Os, Re). The metal complexes will then be investigated for transfer hydrogenation of ketones and production of secondary alcohols. With successful completion of these studies, synthesis of a new chiral PNHN ligand will commence (Scheme 1.16, **eq. 1.7**). The new chiral ligand will be coordinated with the previously mentioned transition metals. These metal complexes will then be employed for asymmetric hydrogenation of ketones and the production of chiral secondary alcohols.

Scheme 1.16

"PNN" ligand   "PNHN" ligand   **eq. 1.6**

"Chiral PNHN" ligand   **eq. 1.7**

23
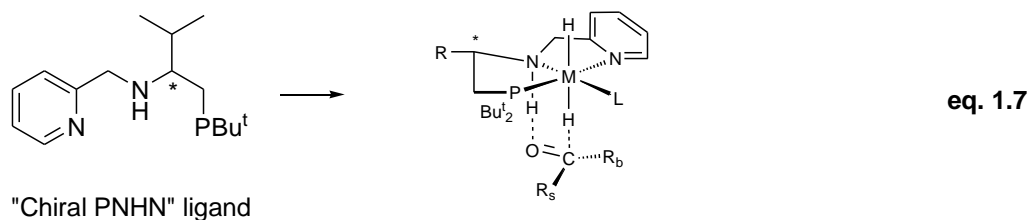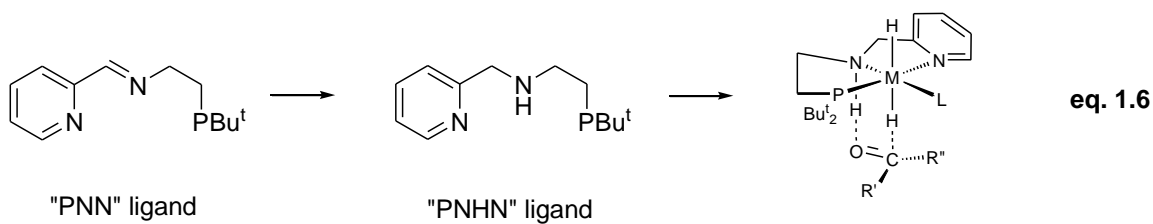
Chapter 2

2.1 Preparation of New Pincer-Type Ligand

The first attempt toward the synthesis of the new PNHN ligand involved a condensation reaction between 2-pyridine-carboxaldehyde and 2-chloroethanamine (Scheme 2.1).

Scheme 2.1

(**2.1**)   (**2.2**)   (**2.3**) 91 %
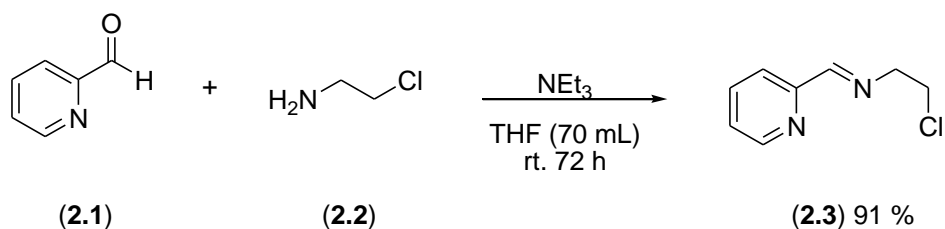
In this reaction the product observed by NMR was (E)-2-chloro-*N*-((pyridine-2-yl)methylene)ethanamine (**2.3**). This was confirmed by ^{13}C {^{1}H} NMR through the disappearance of the C=O peak at 188.9 ppm and the appearance of a peak at 164.6 ppm of the imine carbon. Isolation of the product first required the removal of water produced by this reaction. Removal of water was done to avoid any potential hydrolysis of the imine group regenerating the starting aldehyde **2.1**. Crystallization of the product was accompanied with an impurity present as a singlet at δ 1.35 in the ^{1}H NMR spectrum. Standard purification techniques were unsuccessful in the removal of the impurity. The addition of PBu$^{t}_{2}$ group required reacting **2.3** with lithium di-tert-butylphosphide (Scheme 2.2).

Scheme 2.2

(2.4)

(2.3)

LiPBu$^t_2$

THF
rt. 24 h

PBu$^t_2$

(2.5)
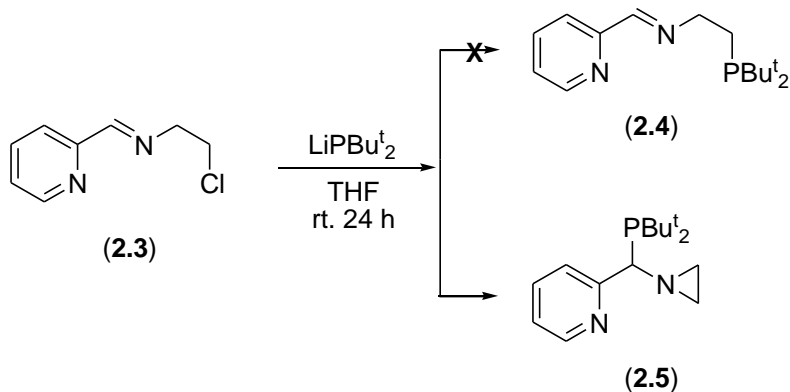
Initial attempts at synthesizing the PNHN ligand (**2.4**) resulted in the formation of an aziridine (**2.5**). The formation of the aziridine is believed to occur through a nucleophilic attack by the PBu$^t_2$ on the electrophilic carbon of the imine. This attack is followed by a second nucleophilic attack by the resulting amide on the carbon bonded to the chlorine resulting in the loss of the chlorine. A doublet at δ 75.9 in the ^{13}C {^{1}H} NMR and an overlapped singlet at δ 3.39 in the ^{1}H NMR spectrum supports the formation of the aziridine. Attempts to avoid this formation involved the addition of LiPBu$^t_2$ to the reaction solution at -80 °C and using ClPBu$^t_2$ in the presence of Li or Zn. In both cases the competing attack on the imine forming the aziridine was more favourable than the desired reaction.

To avoid the formation of **2.5**, it was decided to start with the addition of PBu$^t_2$ to **2.2**. The synthesis required protection of the nitrogen to avoid any reactivity between LiPBu$^t_2$ and the NH$_2$ group (Scheme 2.3).[41] To overcome this problem two TMS groups were used as protecting groups on the nitrogen.

Scheme 2.3

$$\underset{\textbf{(2.2)}}{\overset{\overset{\displaystyle HCl}{\bullet}}{H_2N}\diagdown\diagup\diagup^{Cl}} \quad \xrightarrow[\substack{NEt_3\ (3.3\ equiv.)\\ CH_2Cl_2\ (300\ mL)\\ 1)\ 0\ ^\circ C\\ 2)\ rt.\ 72\ h}]{TMSCl\ (2.2\ equiv.)} \quad \underset{\textbf{(2.6)}\ 64\ \%}{\overset{TMS}{\underset{TMS}{\diagdown}}N\diagup\diagup^{Cl}}$$
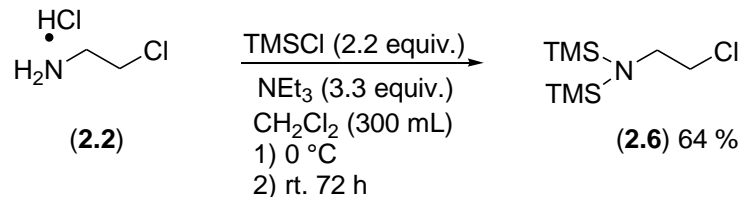
Protection of the nitrogen gave the product **2.6** as a clear colourless liquid with a 64 %
yield. Additionally the protection of the nitrogen competes with self-alkylation and
alkylation between two molecules of **2.2**, even when the reaction is done at low
temperature. Attempts to optimize the reaction have shown no increase in the amount of
recovered product. ^{1}H NMR showed a singlet at δ 0.02 representing the two TMS
protecting groups on the nitrogen and no evidence of the NH_2 group. Addition of PBu^t_2
was achieved by reacting **2.6** with $LiPBu^t_2$ (Scheme 2.4).

Scheme 2.4

$$\underset{\textbf{(2.6)}}{\overset{TMS}{\underset{TMS}{\diagdown}}N\diagup\diagup^{Cl}} \quad \xrightarrow[\substack{THF\ (60\ mL)\\ 1)\ -35\ ^\circ C,\ 30\ min\\ 2)\ rt.\ 3\ h\\ 3)\ reflux\ 1\ h\\ 4)\ H_2O\ (40\ mL)}]{LiPBu^t_2\ (1.8\ equiv.)} \quad \underset{\textbf{(2.7)}}{\overset{TMS}{\underset{TMS}{\diagdown}}N\diagup\diagup^{PBu^t_2}}$$
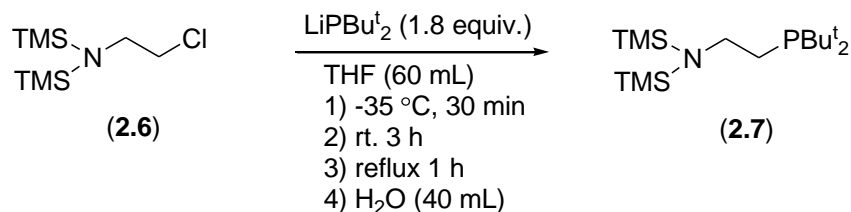
Preparation of $LiPBu^t_2$ was achieved by the addition of $ClPBu^t_2$ to a suspension of
lithium granules in THF with stirring for 72 h. With the reaction flask in a cold bath, **2.6**
was added dropwise to the $LiPBu^t_2$/THF solution. Precautions had to be taken due to the
exothermic nature of this reaction. Water was then used to quench the reaction. The
resulting protected amino phosphine (**2.7**) was isolated with ca. 15 mol% of the $(PBu^t_2)_2$
dimer contaminate visible at δ 40.6 in the ^{31}P {^{1}H} NMR spectrum.

The first attempt at deprotection of the amino phosphine was done employing
TBAF (Scheme 2.5). It is well known that thermal decomposition of TBAF produces *n-*

butene and tributylamine hydrofluoride.[42] This decomposition occurs by E2 elimination where the fluoride ion acts as a strong base. Removal of these impurities was unsuccessful due to the similarities in the boiling points and solubility of tri-n-butylamine and **2.8**. The presence of tri-n-butylamine was visible in the ^{1}H NMR spectrum at δ 2.35 as a triplet. The ^{13}C {^{1}H} NMR spectrum showed single peaks at δ 54.3, 29.8, 20.9 and 14.3 all belonging to tri-n-butylamine.

Scheme 2.5
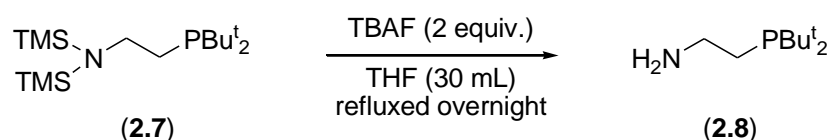
To avoid contamination by tributylamine, alternative deprotecting agents were employed. The use of Me$_4$NF, Et$_4$NF and NH$_4$F was. In all cases no evidence of deprotection was observed. Since the decomposition of TBAF and formation of HF in the reaction mixture was responsible for the deprotection of **2.7**, it was decided to use triethylamine trihydrofluoride for deprotection (Scheme 2.6).

Scheme 2.6
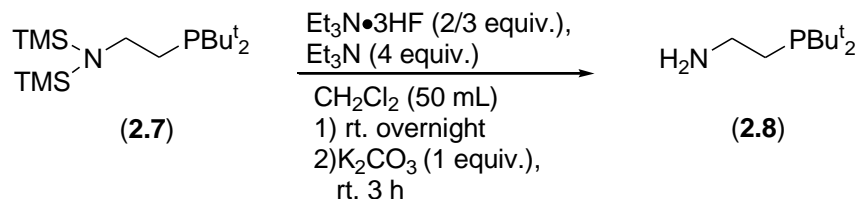
After stirring at room temperature overnight, K$_2$CO$_3$ was added to help isolate **2.8**. Analysis of the ^{1}H NMR spectrum confirmed the removal of the protecting groups and a new singlet at δ 3.42 for the NH$_2$ group. Isolation of **2.8** resulted in a clear colourless liquid with a yield of 77 %. The completion of the ligand backbone called for a condensation reaction between **2.8** and **2.1** (Scheme 2.7).

Scheme 2.7

(**2.1**)   (**2.8**)   (**2.4**) 96 %
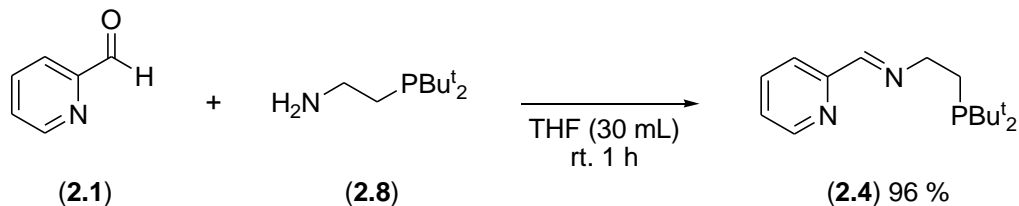
1.1 equivalents of **2.1** were added dropwise to the reaction solution over 5 min.
Continuous stirring at room temperature over 1 h afforded the PNN ligand **2.4**.
Evaporation under vacuum gave the product as a clear dark orange oil at near quantitative
yield (96 %). Characterization using NMR techniques showed the presence of **2.4**. Before
attempting to reduce the imine group, coordination chemistry using **2.4** was investigated.

2.2 Coordination of PNN Ligand to Ir and Ru

As reported by Del Zotto and Baratta, complexes with a ligand system such as
2.4 have been shown to demonstrate high activity toward transfer hydrogenation.
Reduction of the imine would be accomplished through activation of the catalyst. With
the ligand **2.4** in hand, coordination chemistry was done by employing the transition
metals Ir and Ru. Initial attempts of coordination with Ir were done using $[IrCl(COE)_2]_2$
(Scheme 2.8) and $IrCl_3 \cdot 3H_2O$ (Scheme 2.9).

Scheme 2.8

(**2.4**)

(**2.9**)
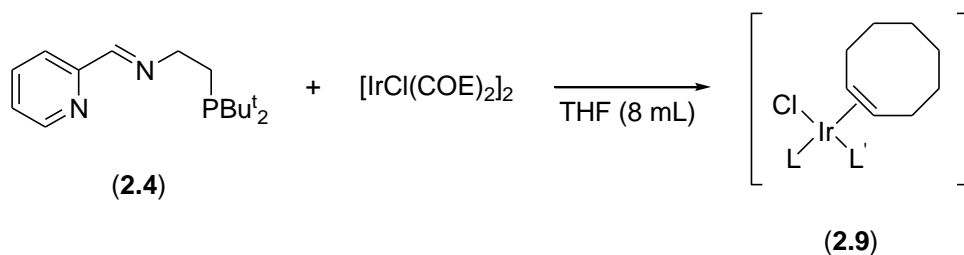
The reaction between **2.4** and [IrCl(COE)$_2$]$_2$ was done using 0.45 equivalents of the Ir dimer. The expected structure would be formed through a cleavage of the dimer followed by displacement of one cyclooctene (**2.9**). The groups L and L$^{'}$ each represent one of either nitrogen group or the phosphorus group of **2.4**. The reaction produced a precipitate which was believed to be **2.9** since the solution contained no evidence of the phosphorus group. Characterization of the precipitate was not completed due to poor solubility. Coordination of **2.4** was then attempted using IrCl$_3$·3H$_2$O.

Scheme 2.9
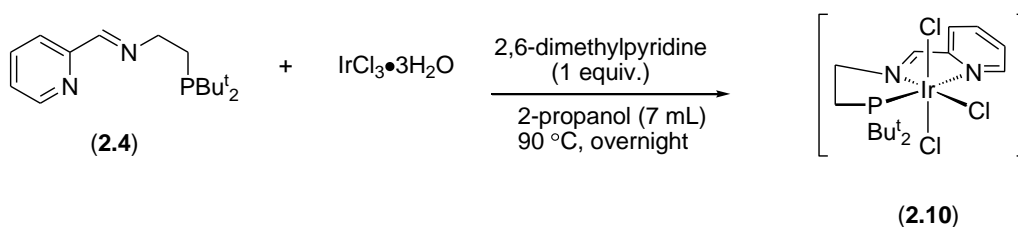
The first attempt of the reaction in Scheme 2.9 was done under N$_2$ and left stirring overnight. With the completion of the reaction a precipitate formed. NMR showed that the reaction solution again contained no phosphorus. Again any attempts to characterize the solid were unsuccessful due to poor solubility. Since it is know that N$_2$ can react with Ir complexes, the reaction was repeated under H$_2$. Characterization was not completed due to poor solubility.

Coordination of **2.4** with Ru was then attempted using [RuCl$_2$(p-cymene)]$_2$ (Scheme 2.10, **eq. 2.1**) and RuCl$_2$(PPh$_3$)$_3$ (Scheme 2.10, **eq. 2.2**).

Scheme 2.10

(2.4)   +   [RuCl$_2$(p-cymene)]$_2$ $\xrightarrow[\substack{C_6H_6 \text{ (7 mL)} \\ 68\,^\circ C,\text{ overnight}}]{H_2}$ (2.11)   **eq. 2.1**

(2.4)   +   RuCl$_2$(PPh$_3$)$_3$ $\xrightarrow[\substack{\text{Toluene (7 mL)} \\ 90\,^\circ C,\text{ 1 h}}]{}$ (2.12)   **eq. 2.2**
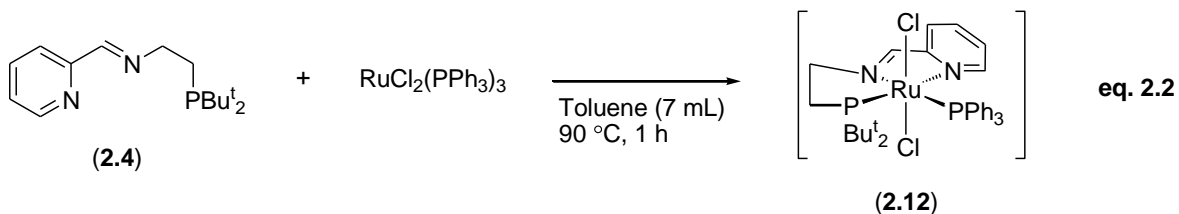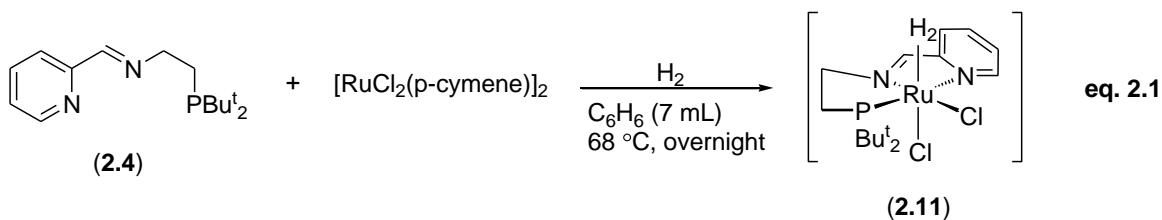
Shown in the square brackets are the proposed structures of the resulting ruthenium complexes (Scheme 2.10). As was the case with Ir, the solubility of the expected products did not allow for proper characterization. Varying the reaction conditions of the Ir and Ru coordination reactions showed no improvement with the solubility of the complexes. It was decided the reduction of the imine group in **2.4** before coordination could improve the solubility of the metal complexes.

2.3 PNHN Ligand

Reduction of the imine group would result in the formation of the protic hydrogen required for the bifunctional mechanism. Reduction of the imine group employing a number a reducing agents (NaBH$_4$, LiAlH$_4$, Super hydride, lithium aluminum tri-*tert*-butoxy hydride, Pt/c, Pd/c and Raney-Ni) showed reduction of the imine but eventually DIBAL-H (Scheme 2.11) was used because of more convenient isolation/purification of the reduced product.

Scheme 2.11

(2.4)   (2.13)
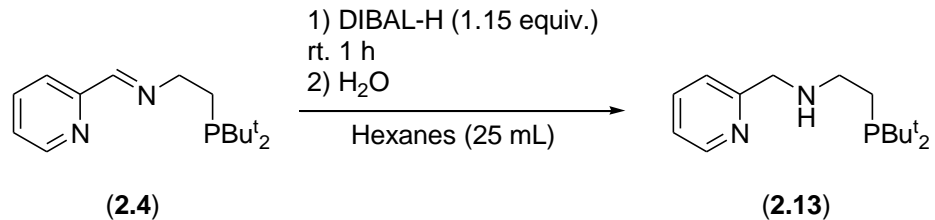
Simply quenching the reaction with water resulted in **2.13** which was isolated by removing the precipitate using filtration and evaporation of the solvent. The resulting PNHN ligand was obtained as a clear light orange oil with a yield of 91 %. With this new ligand in hand coordination chemistry with Ir and Ru was revisited.

Chapter 3

The Bu^t groups of all Ir metal complexes have been omitted for clarity reasons.

3.1 Iridium Chloride

Equal amounts of **2.13** and [IrCl(COE)$_2$]$_2$ were dissolved in toluene and left stirring under nitrogen for 30 min. The nitrogen was then evacuated and replaced with H$_2$ gas through a series of freeze-pump-thaw cycles. The H$_2$ gas is used as the hydride source. After 1 h of stirring under H$_2$, the reaction solution was left overnight. This resulted in the displacement of cyclooctene and the formation of a new complex containing the coordinated PNHN ligand (Scheme 3.1).

Scheme 3.1

(**2.13**)   [IrCl(COE)$_2$]$_2$ (1 equiv.)   Toluene (5 mL)   (**3.0**)
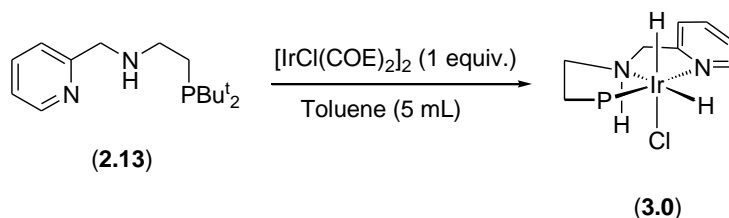
The product was obtained as a pale green solid with the presence of residual solvent. Characterization was done using ^{1}H and ^{31}P {^{1}H} NMR. The product was difficult to characterize by ^{13}C {^{1}H} NMR due to poor solubility. From the ^{1}H NMR spectrum, the doublet at δ 9.08 was indicative of the CH-N fragment in the pyridine ring. The remaining CH groups a multiplet at δ 7.72, a doublet at δ 7.26 and a triplet at δ 7.17. The distinct downshift of the CH-N resonance is believed to be caused by the coordination of the nitrogen to the metal center. Due to the C$_1$ symmetry of **3.0** all CH$_2$ protons of the PNHN ligand are magnetically inequivalent. NOE decoupling revealed that the broad singlet belonged to the NH group coordinated to the metal center. This experiment identified the CH$_2$ groups bound on either side of the NH. The ^{1}H NMR spectrum showed

doublets of doublets at δ 4.81 and 3.99 of the CH_2 bonded to pyridine and the central nitrogen. The multiplets at δ 3.54 and 2.59 belong to the other CH_2 group bonded to the central nitrogen. Finally, the CH_2 group bonded to phosphorus was identified by the doublet of doublets at δ 2.33 and the multiplet at δ 2.06. The shifts for the Bu^t groups on phosphorus showed as a doublet at δ 1.32 in the ^{1}H NMR spectrum due to overlap of the Bu^t resonances. Finally the metal complex exhibited hydride resonances at δ -19.89 and -25.28 as doublets of doublets. The coupling constants between the hydrides and phosphorus are $^2J_{HP}$ = 17.7 Hz and 21.9 Hz. The coupling constant between the hydrides is $^2J_{HH}$ = 7.5 Hz which is typical for hydrides *cis* to each other. The IR spectrum of **3.0** showed a band at 3363 cm^{-1} due to the N-H stretch and two strong bands at 2273 cm^{-1} and 2185 cm^{-1} for the Ir-H vibrations. The ^{31}P {^{1}H} NMR spectrum showed a singlet at δ 54.0 of the coordinated phosphorus. Interestingly all reactions performed also showed accompanying isomers of the desired product. From the ^{1}H NMR spectrum shifts which were slightly shifted and similar to the major product were visible. The resonances at δ -21.39 and -23.42 in the hydride region belonged to an isomer of the major product. The ^{31}P {^{1}H} NMR spectrum showed a singlet at δ 63.2 also belonging to the isomer. DFT calculations suggested that there are three possible isomers of the expected product. The isomers are meridional syn $IrCl(H)_2(PNHN)$ (Figure 3.1, **3.0**), meridional anti $IrCl(H)_2(PNHN)$ (Figure 3.2, **3.1**) and facial $IrCl(H)_2(PNHN)$ (Figure 3.3, **3.2**). The calculated enthalpies of the isomers are 0 kcal/mol for **3.0**, 1.3 kcal/mol for **3.1** and 5.1 kcal/mol for **3.2**. The relatively low energies of **3.0** and **3.1** further supports their presence. The enthalpy for **3.2** is high enough to suggest that this isomer would not be

expected to form. In the accompanying diagrams most of the hydrogen atoms have been

omitted from the calculated structures for clarity purposes.
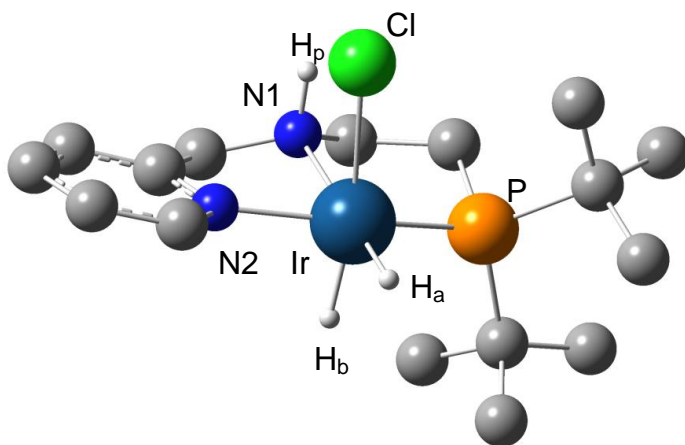
Figure 3.1

Figure 3.1 illustrates the DFT structure representing the meridional syn

$IrCl(H)_2(PNHN)$ complex. The PNHN ligand defines the plain. The hydride H_a is shown

in the plain and *trans* to the central nitrogen (N1). The second hydride H_b is *trans* to the

chloride (Cl). The two Bu^t groups on the phosphorus (P) are slightly bent away from the

chlorine atom due to a slight steric interaction. The main structural feature is that the

chlorine atom and the protic hydrogen are on the same side of the plain thus located syn

to each other.
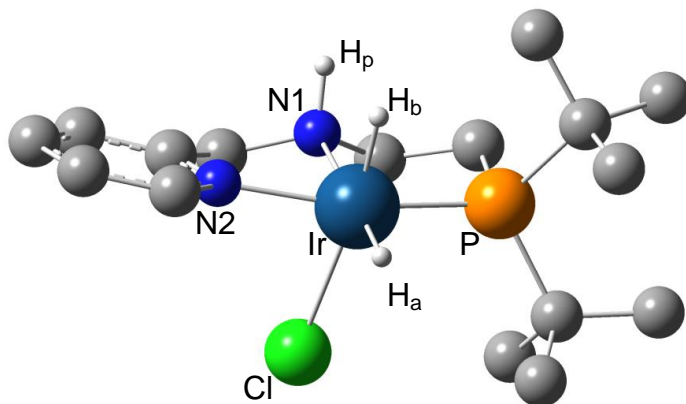
Figure 3.2)

The second isomer shown in Figure 3.2 represents the DFT calculation structure of the meridial anti IrCl(H)$_2$(PNHN) metal complex. Again the PNHN ligand defines the plain. The hydride H$_a$ is *trans* to the central nitrogen (N1). The two Bu^t groups are seen slightly bent away from the chloride because of sterics. The second hydride H$_b$ and the protic hydrogen H$_p$ are located on the same side of the plain. With this complex the chloride is now positioned anti to the protic hydrogen.

3.2 Iridium Dihydride

Previous synthesis of iridium complexes (**3.3**) done in our group used KOBu^t to perform the dehydrochlorination affording the amido complex **3.4** (Scheme 3.2, **eq. 3.1**).[43] Further reactivity of the amido complex under 1 atm of H$_2$ gave the trihydride (**3.5**) used for catalysis (Scheme 3.2, **eq. 3.2**).[43]

Scheme 3.2

eq. 3.1

(3.3)   (3.4)

eq. 3.2

(3.4)   (3.5)
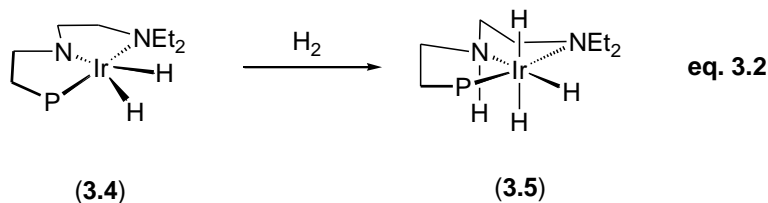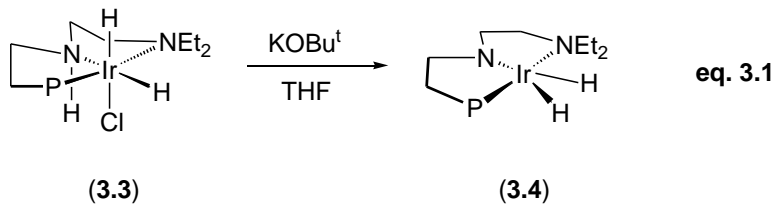
Initially synthesis of the trihydride from the isomers **3.0** and **3.1** was attempted using the same process outlined in **eq. 3.1** and **eq. 3.2**. Unfortunately there was no formation of the desired hydride complex **3.5**. Instead of KOBu^t, Super hydride was employed to perform reduction and produce the trihydride **3.5** (Scheme 3.3).

Scheme 3.3

(3.0)   (3.5)
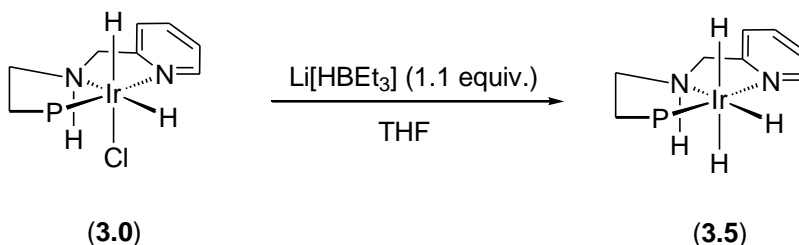
The reaction solution turned pale yellow after 1 h stirring at room temperature. Characterization using ^{1}H NMR and ^{31}P {^{1}H} NMR revealed the formation of the trihydride along with the amido complex shown in Figure 3.4. The presence of the amido complex is possibly due to loss of H$_2$.[43] Separation of **3.5** or **3.6** for characterization purposes was achieved. The ^{1}H NMR spectrum showed hydride shifts at δ -8.48 and -8.97. These hydride shifts belong to H' and H" of complex **3.5** (Figure 3.4). The hydride shift at δ -16.78 belongs to the hydride *trans* to the central nitrogen. The apparent

36

symmetry of **3.6** is C$_s$ where the PNN atoms define the ligand plain. Thus the two Bu^t and

two hydrides are pairwise equivalent in the NMR spectra as well as the hydrogens of the

CH$_2$ groups in the PNHN ligand backbone. Analysis of ^{1}H NMR spectrum showed a shift

at δ -23.59 for the hydrides of **3.6** (Figure 3.4). Due to the poor solubility of complexes

3.5 and **3.6**, further characterization was incomplete. Analysis of the ^{31}P {^{1}H} NMR

showed a shift at δ 63.8 of the phosphorus group of **3.6** and δ 57.6 of the phosphorus

group of **3.5**.

(**3.5**)   (**3.6**)
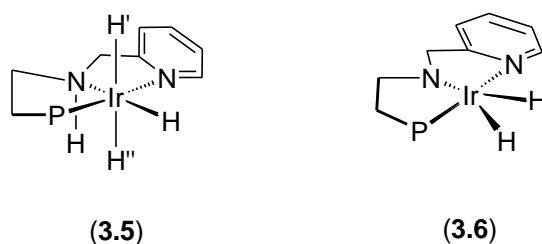
Figure 3.4

Since separation was incomplete, catalysis was performed using a solution

containing both complexes. Complexes **3.5** and **3.6** were tested for hydrogenation of

representative ketones using ^{1}H NMR to monitor the reactions. A mixture of **3.5** and **3.6**

in THF reacted with acetophenone and cyclohexanone at room temperature in 2-propanol

showed no hydrogenation. Due to the poor solubility of the complexes and the inactivity

towards catalysis, attention was turned to synthesis of ruthenium complexes for

hydrogenation of ketones.

Chapter 4

The Bu^t groups of all Ru metal complexes have been omitted for clarity reasons.

4.1 Ruthenium Dichloride

4.1.1 Synthesis using [RuCl$_2$(p-cymene)]$_2$

Initial preparation of the ruthenium chloride represented by the proposed structure **4.1** was done using the starting complex [RuCl$_2$(p-cymene)]$_2$. Equal amounts of the PNHN ligand and [RuCl$_2$(p-cymene)]$_2$ in the presence of 4 equivalents of 2, 6-lutidine were dissolved in 2-propanol. The reaction solution was heated overnight at 90 ^{o}C with stirring (Scheme 4.1). The resulting product was formed as clear reddish platelet crystals. Isolation of the crystals was done by decanting and drying under vacuum. ^{1}H NMR analysis was not completed due to poor solubility of the crystals. The ^{31}P {^{1}H} NMR did show the formation of a ruthenium complex at δ 99.8.

Scheme 4.1

(**2.13**)   (**4.1**)
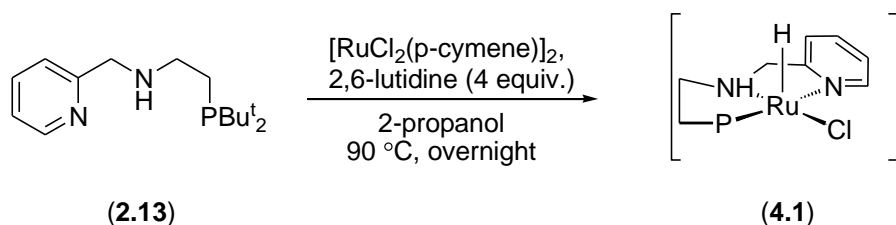
To improve the solubility of the product, the crystalline material was used to prepare the proposed ruthenium hydride **4.2**. Preparation of the ruthenium hydride was attempted by using KOBu^t (Scheme 4.2) and Bu$_4$NBH$_4$ (Scheme 4.2) under argon to obtain the ruthenium hydride.

Scheme 4.2

(**4.1**)   (**4.2**)
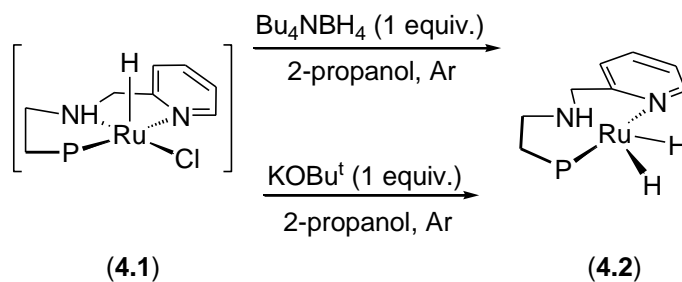
Analysis of ^{31}P $\{^1H\}$ NMR for the reaction using Bu_4NBH_4 showed the formation of a mixture of products. The ^{31}P $\{^1H\}$ NMR for the reaction using $KOBu^t$ showed the formation of one major product at δ 112.5. The ^1H NMR showed a broad hydride shift at δ -16.69 representing the equivalent hydrides of the expected metal complex. Since the product had low solubility in THF, complete characterization of the complex was not achieved. There was also no indication of the protic hydrogen. Attempts at producing a *tetra* hydride species (**4.3**) by performing the reaction using $KOBu^t$ under H_2 gas (Scheme 4.3) resulted in multiple shifts in the hydride region on the ^1H NMR spectrum.

Scheme 4.3

(**4.1**)   (**4.3**)
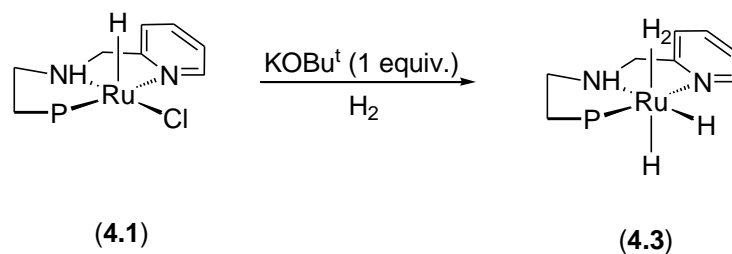
4.1.2 Synthesis using $RuCl_2(PPh_3)_3$

With the unsuccessful synthesis of the ruthenium chloride (**4.1**) using $[RuCl_2(p$-cymene)]_2$, attention was turned to using $RuCl_2(PPh_3)_3$ as the starting complex for the synthesis of a ruthenium dichloride complex. The PNHN ligand and $RuCl_2(PPh_3)_3$ were

dissolved in toluene and left stirring for 3 h under nitrogen. Isolation of the resulting light orange coloured solid afforded the ruthenium dichloride **4.4** with a yield of 89 % (Scheme 4.4).

Scheme 4.4

(**2.13**)   (**4.4**)
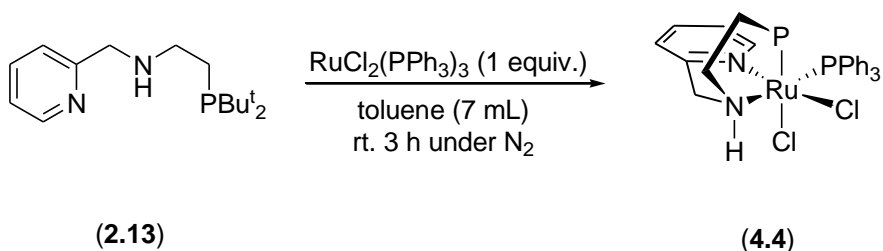
With the improved solubility of **4.4**, analysis of the ^{31}P $\{^{1}$H$\}$ and ^{1}H NMR provide clear information about the structure of the dichloride. The ^{31}P $\{^{1}$H$\}$ NMR spectrum showed two doublets, one at δ 52.9 and the other at δ 40.1. The two-bond coupling constant of $^{2}J_{PP}$ = 21.1 is indicative of two phosphorus groups *cis* to one another. The structural conformation of the ligand was determined to be facial with the PBu$^{t}_{2}$ group located above the metal centre and *trans* to one of the chlorides. The correct structure of the complex was not determined due to the difficulties of growing crystals for XRD analysis. The facial configuration is supported by ^{1}H NMR data. Examination of the ^{1}H NMR spectrum of **4.4** revealed a unique shift at δ 8.50 and further downshifted from the rest of the pyridine shifts. Analysis using NOE showed that the shift was of the proton C*H*-N group of the pyridine ring. This unique shift also showed an interaction with protons from the triphenylphosphine group found at δ 7.08, interaction with the NH group found at δ 5.78 and with the PBu$^{t}_{2}$ groups at δ 1.22. This information along with the ^{31}P $\{^{1}$H$\}$ NMR spectrum provides the necessary information to suggest that the phosphorus groups are *cis* and that the triphenylphosphine group is *trans* to the central nitrogen. Further investigation of the ^{1}H NMR spectrum provided information supporting the expected C$_1$

symmetry of the complex through the magnetically inequivalent hydrogens of the CH_2 groups of the PNHN ligand. Due to the difficulties with solubility, proper ^{13}C {^{1}H} NMR analysis could not be performed. The IR spectrum shows a peak at 3186 cm^{-1} of the NH group. With the synthesis of the dichloride preparation of the dihydride began.

4.2 Ruthenium Dihydride

Initial attempts toward the synthesis of the ruthenium dihydride complex employed Super hydride. One equivalent of Super hydride was added to the ruthenium dichloride **4.4** in 2-propanol. The ^{31}P {^{1}H} NMR showed multiple peaks with two major ones representing the wanted hydride species. The ^{1}H NMR spectrum only showed hydride shifts belonging to the product. Unfortunately attempts at isolation were ineffective. Attention turned to previous synthesis of dihydrides performed in our group with the use of KOBu^{t} and 2-propanol (Scheme 4.5). The final dihydride complex **4.5** is a result of transfer hydrogenation from 2-propanol to the ruthenium complex.

Scheme 4.5

(4.4)   (4.5)
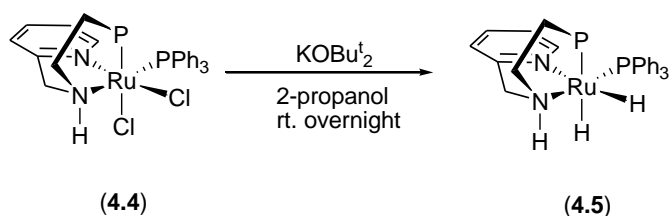
Upon addition of KOBu^{t} the resulting solution turned a dark green colour. After 1 h of stirring at room temperature the reaction mixture turned a dark brownish-orange. After stirring overnight a fine light orange precipitate formed. Isolation was achieved with evaporation of the solvent and drying under vacuum. The product precipitate was too fine to filter for isolation. The ^{31}P {^{1}H} NMR spectrum showed the formation of two

complexes. The major complex showed doublets at δ 104.0 and δ 69.4. The coupling constants were $^2J_{PP}$ = 291.6 Hz for both doublets. The large coupling constant is indicative of two phosphorus groups located *trans* to each other. The minor complex has doublets at δ 79.8 and δ 78.9. The coupling constant is $^2J_{PP}$ = 7.1 Hz for both doublets. The relatively small coupling constant is a result of the two phosphorus groups located *cis* to each other. The ^{1}H NMR spectrum showed two multiplets in the hydride region at δ -18.02 and δ -18.51 belonging to the major species. There was also a multiplet at δ -16.43 which belonged to the minor species. Analysis of the hydride region showed the presence of a dihydride and what appeared to be a monohydride species. Due to residual solvent from the reaction and washing, proper characterization could not be done on the sample prepared in 2-propanol. The reaction was repeated but with 2-pentanol as the solvent. With 2-pentanol the solubility of the complexes decreased allowing for better isolation of the product. A similar procedure was followed using 2-pentanol instead of 2-propanol. The product was obtained as a brownish orange solid with a minimal amount of residual 2-pentanol and potassium chloride. Decoupling experiments on the ^{31}P {^{1}H} NMR spectrum showed that the doublet at δ 104.0 belonged to the PBu$^t_2$ group and the doublet at δ 69.4 belonging to the PPh$_3$ group. The ^{1}H NMR spectrum again showed the aforementioned chemical shifts in the hydride region as multiplets. The symmetry of the dihydride is C_1 and thus the hydrogens of the CH$_2$ groups are magnetically inequivalent. With the use of standard NMR techniques it was determined that the two products obtained were both dihydrides illustrated in Figure 4.1.
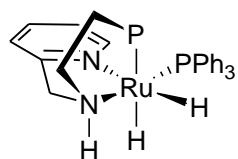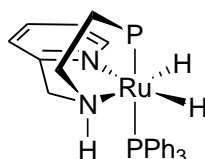
(4.5)   (4.6)

Figure 4.1

In the reaction using 2-propanol it was believed that the minor product was a monohydride species. With the use of 2-pentanol complete characterization of both species revealed that the minor species was the dihydride complex **4.5** and the major complex was **4.6**. The ^{1}H NMR spectrum now showed a multiplet at δ -7.72 and at δ -16.43 both belonging to the minor dihydride complex. The DFT calculated structure shown in Figure 4.2 depicts complex **4.5**.
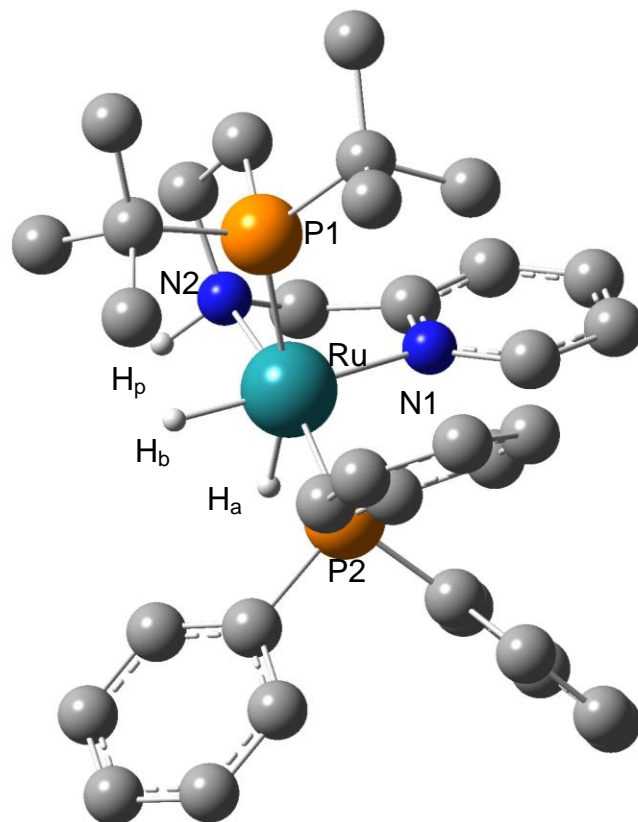
Figure 4.2

The DFT calculated structure of the minor complex shows the two phosphorus groups (P1 and P2) *cis* to each other. The triphenylphosphine group (P2) is located *trans* to the central nitrogen (N2) and the PBu^t_2 group (P1) is located *trans* to the hydride H_a. This structure also shows the location of the hydrides (H_a and H_b) *cis* to one another. The hydride H_b is located *trans* to the nitrogen (N1) of the pyridine ring. This results in an overall facial structure of the ruthenium dihydride complex with atoms N1, N2, P2 and H_b all in the same plain and P1 located above the plain. Figure 4.4 illustrates the DFT calculated structure for the major dihydride complex.
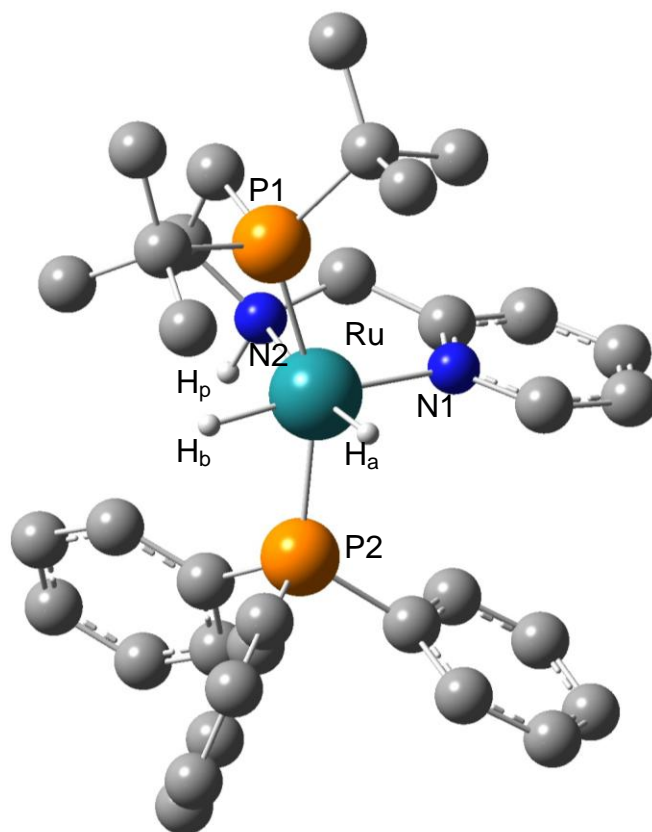
Figure 4.3

The DFT calculated structure for the major dihydride shows the two phosphorus (P1 and P2) groups *trans* to each other. The phosphorus groups (P1 and P2) are located above and below the metal center. As with the minor ruthenium dihydride, the hydrides are also located *cis* to one another. The difference being that H_a is now *trans* to the central nitrogen (N2) instead of the triphenylphosphine group (P2).

To fully characterize the complexes, crystals were grown through slow diffusion of hexane into a solution of toluene containing the ruthenium dihydride complexes. The resulting crystal structure, of the major dihydride, is illustrated in Figure 4.4. Due to the quality of the crystals no meaningful bond angles or bond lengths could be obtained from

the crystal structure. The difficulty with improving the crystal structure is believed to be caused by interference from the minor dihydride.
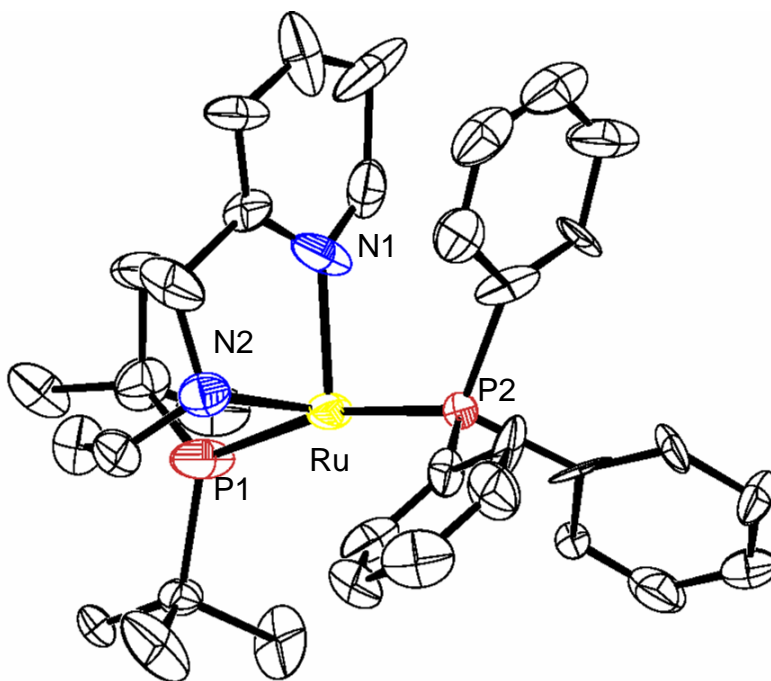
Figure 4.4
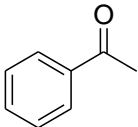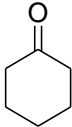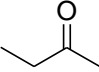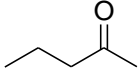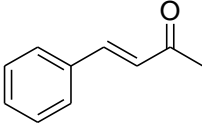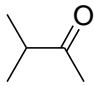
With both structures fully characterized, the complexes were then used in catalysis reactions.

4.2.1 Transfer Hydrogenation of Ketones

An NMR tube reaction mixture (S:C = 250:1) containing acetophenone (300 mg), 2-propanol (1 mL) and catalytic amounts of the ruthenium dihydride (6 mg) showed reasonable transfer hydrogenation of the ketone to the expected 2-phenylethanol at room temperature without the addition of a base. Due to the limited solubility of the dihydride in 2-propanol, a solution of acetophenone and 2-propanol was prepared first followed by the addition of the dihydride. As catalysis proceeded, the dihydride dissolved. Attempts

to improve catalysis resulted in similar results. The results of catalysis are shown in Table 4.1.

Table 4.1

Substrate	Temp. (^{o}C)	S:C	Time (min)	Conv. (%)
	25	250	40	54
	25	250	45	81
	25	250	60	<10
	25	250	60	<10
	25	250	60	N. R.
	25	250	60	N. R.

In the first two cases formation of 2-phenylethanol and cyclohexanol where observed by ^{1}H NMR. Cases three and four showed less than 10 % formation of the secondary alcohol while cases five and six showed no reactivity. It can be concluded that the catalytic activity of the ruthenium dihydride complex is low. In an attempt to better

understand the reactivity of the dihydride, isolation of the resulting amido complex after transfer hydrogenation of the ketone was attempted.

4.2.2 Ruthenium Amido Complex

      With both the bifunctional mechanism, the transfer of the hydridic and protic hydrogens to the ketone forms a 16-electron amido complex. The inner-sphere mechanism involves the coordination of a ketone to an empty coordination site on the metal complex. This complex is usually reduced by an alcohol solvent to regenerate the starting catalyst. To better understand why the catalysis employing the ruthenium dihydride is not efficient, isolation of the amido complex was attempted.

      In a J. Yung NMR tube the ruthenium dihydride was dissolved in THF. Freeze-pump-thaw cycles were performed every 30 min with intermittent heating at 50 ^{o}C for 5 min periods. By placing the ruthenium dihydride under vacuum, H_2 was slowly liberated forming the 16-electron amido complex (Scheme 4.6).

Scheme 4.6

         (**4.6**)   (**4.7**)
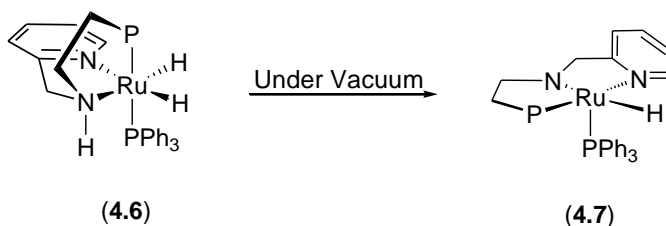
With the liberation of the H_2 molecule from the ruthenium dihydride, a structural change occurred resulting in the phosphorus groups now located *cis* to each other with the ligand backbone now meridial. The purpose of this experiment was to gain a better understanding of the structural nature of the 16-electron complex. The resulting amido complex was obtained in solution with a conversion of 70 %. This change in the

complexes geometry was confirmed with the ^{31}P {^{1}H} NMR spectrum. The phosphorus

shifts were now located at δ 109.8 and δ 73.8 as doublets. The coupling constant for the

new phosphorus shifts is $^{2}J_{pp}$ = 16.5 Hz respectively which is indicative of phosphorus

groups *cis* to each other. The ^{1}H NMR spectrum showed the presence of a doublet of

doublets at δ -19.52 representing the hydride of the amido complex. Exploration into the

removal of the triphenylphosphine group and replacing it with a carbonyl group was

investigated. The replacement of the triphenylphosphine group with the carbonyl group

could improve the catalytic ability of the dihydride.

4.3 Ruthenium Carbonyl Complex

In order to improve the catalytic activity of the ruthenium dihydride an alternative

synthesis involving a carbonyl group in place of the triphenylphosphine was implemented.

Morales-Morales and coworkers developed the following synthesis to replace one of the

triphenylphosphine groups of RuCl$_2$(PPh$_3$)$_3$ with a carbonyl group (Scheme 4.7).[44,45]

Scheme 4.7

(**4.8**)
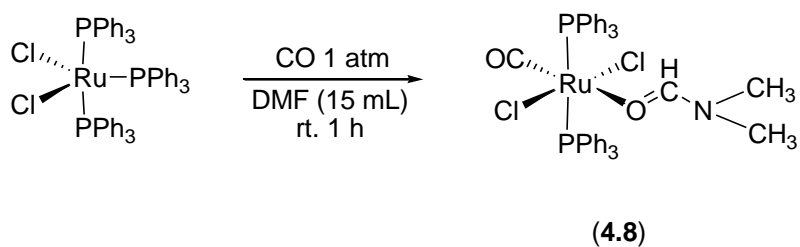
Addition of the carbonyl ligand is interesting due to its sensitivity to electronic density

changes and the relative ease for identification of the carbonyl group through NMR and

IR techniques. By simply stirring a solution of RuCl$_2$(PPh$_3$)$_3$ in DMF under carbon

monoxide complex **4.8** is obtained. Complex **4.8** was obtained as a pale yellow solid with

an 83 % yield. From the ^{31}P {^{1}H} NMR spectrum both triphenylphosphine groups

showed as a single shift at δ 35.9. From the ^{1}H NMR spectrum the coordinated dimethylformamide was identified at δ 2.23 as overlapped doublets representing the two methyl groups and at δ 6.81 representing the CH group. Unfortunately the solubility **4.8** did not allow for proper characterization using ^{13}C {^{1}H} NMR. It can however be said with certainty that the complex is the desired complex since the NMR shifts are in reasonable agreement with the reported values. The IR spectrum of **4.8** showed a broad peak at 1913 cm^{-1} belonging to both carbonyl groups.

A solution of **4.8** in glyme was then treated with the PNHN ligand and allowed to stir for 4 h at 90 ^{o}C. The resulting mixture was left stirring at room temperature overnight (Scheme 4.8).

Scheme 4.8

(**4.8**)   (**2.13**)   (**4.9**)
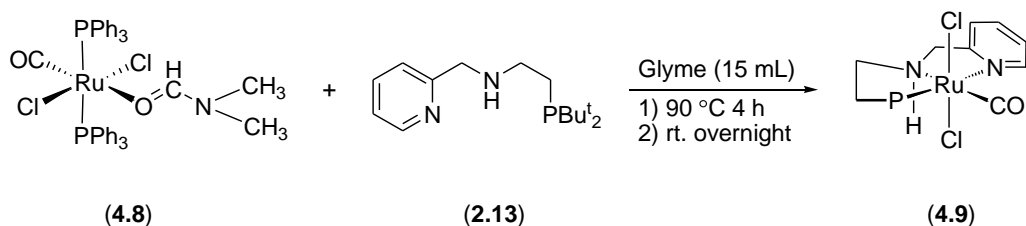
The resulting ruthenium dichloride (**4.9**) was isolated as a yellow solid with a yield of 88 %. The ^{31}P {^{1}H} NMR spectrum showed a singlet at δ 86.5 representing the phosphorus group. The ^{1}H NMR spectrum gave the expected shifts of the pyridine ring with the C*H*-N proton at δ 8.94 downshifted from the other three protons. There was no evidence of coordinated triphenylphosphine. Due to the C_1 symmetry of the complex, the protons of the CH$_2$ groups are magnetically inequivalent. Complete characterization was achieved with the ^{13}C {^{1}H} NMR spectrum where the carbonyl group was visible at δ 203.8 as a doublet. The IR spectrum showed a peak at 1929 cm^{-1} representing the carbonyl group and a peak at 3178 cm^{-1} of the NH group. Interestingly, **4.9** showed high

stability in the polar solvent dimethylsulphoxide. The synthesis of the hydride has not yet been achieved (Scheme 4.9).

Scheme 4.9

(**4.9**)   (**4.10**)   (**4.11**)
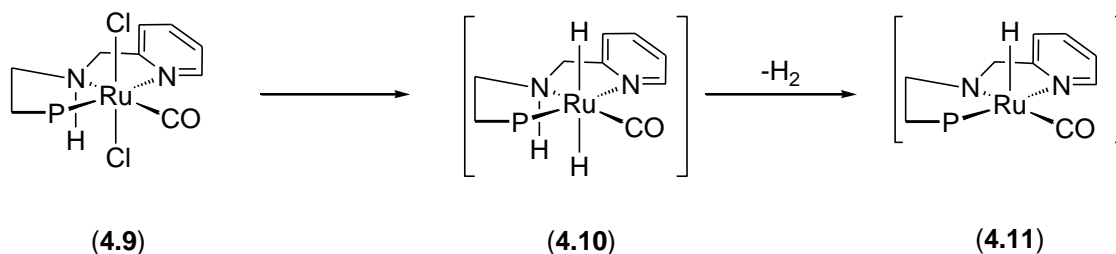
It is believed that the dihydride demonstrates loss of H_2 immediately resulting in a monohydride complex represented by the proposed structure **4.11** (Scheme 4.9). The ^{31}P $\{^{1}$H$\}$ NMR shows a shift at δ 122.4 of what is believed to be the monohydride complex. This is supported by a doublet in the hydride region of the ^{1}H NMR spectrum at δ -17.06. Isolation and complete characterization of the resulting complex has not been accomplished.

Chapter 5

5.1 Chiral PNHN Ligand

Attention turned to the preparation of a new chiral PNHN ligand. The goal was to add an isopropyl group to the CH_2 group on the phosphine side of the central nitrogen. With the addition of the isopropyl group there is potential for improved solubility and asymmetric hydrogenation of various ketones. Addition of the isopropyl group would be achieved by employing commercially available L-valinol. Initial attempts to add the PBu^t_2 group to L-valinol proved unsuccessful. It was decided to use a previously reported synthesis of an amino alcohol (**5.4**) by Cleij and coworkers to prepare the backbone for the chiral PNHN ligand (Scheme 5.1).[46] The asterisk denotes the chiral center for all structures in this chapter.

Scheme 5.1

(**5.1**) (**5.2**) (**5.3**)
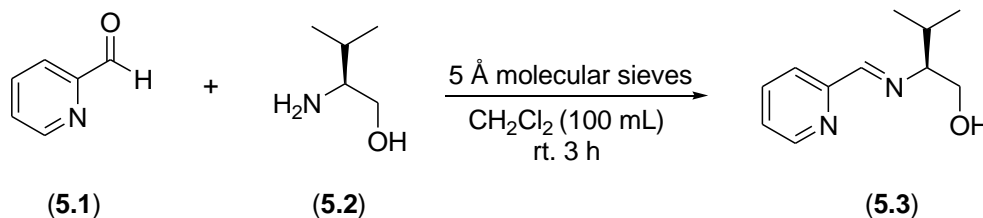
Filtration followed by evaporation of the solvent under vacuum afforded a clear colourless oil containing **5.3**. Reduction of the imine group was done through the reaction of **5.3** with sodium borohydride in ethanol overnight (Scheme 5.2) affording the desired amino alcohol **5.4**.

Scheme 5.2

(5.3)   (5.4)
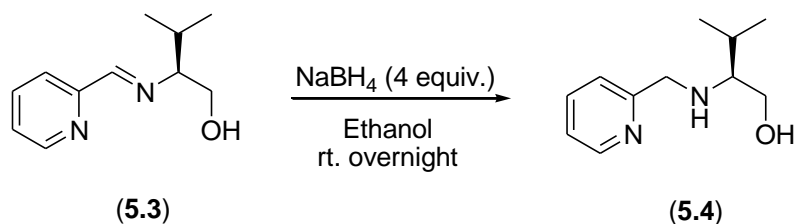
The chiral ligand **5.4** was obtained as a clear pale yellow oil with a 94 % yield. Confirmation of the structure was verified with the presence of the multiplet at δ 2.47 of the CH group bonded to the central nitrogen. The coordinated isopropyl group gave a multiplet at δ 1.82 of the CH group and doublets at δ 0.96 and 0.90 of the CH_3 groups. All other shifts agreed with the reported values. The synthesis continued with the preparation of the amino chloride (**5.5**) seen in Scheme 5.3.

Scheme 5.3

(5.4)   (5.5)
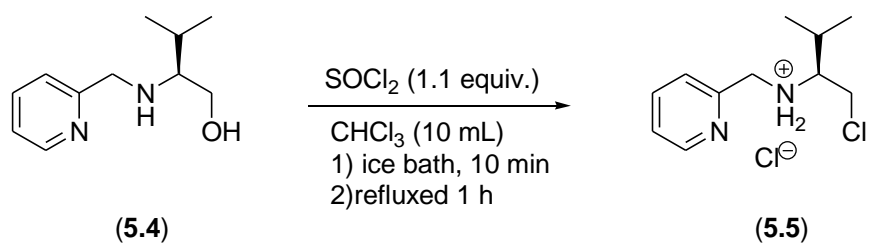
After refluxing for 1 h the resulting amino chloride was filtered and isolated as a beige solid with a yield of 42 %. Due to the poor solubility of **5.5** in chlorinated solvents, DMSO had to be used for proper characterization. The ^{1}H NMR spectrum shows all the expected peaks with the exception of a broad peak at δ 9.98 belonging to the NH_2 group. The shift representing the CH_2 group bonded to the pyridine ring is now a singlet at δ4.57. Finally the addition of the chloride atom to the ligand is confirmed with presence of the multiplet at δ 4.10 of the CH_2Cl group. The ^{13}C {^{1}H} NMR spectrum also confirms the presence of the CH_2Cl group with the appearance of a peak at δ 41.4. Optimization of this

reaction has failed to increase the overall yield of **5.5**. Due to the poor solubility of **5.5** in chlorinated solvents, recovery of the product was done by washing with methylene chloride and filtration. Problems could also be associated with the length of time needed for reflux. Further experimentation is required to determine the proper reaction conditions. With the amino chloride ligand isolated, the addition of the PBu$^t_2$ group was investigated.

As with the synthesis of the PNHN ligand precautions had to be taken to insure no reaction between PBu$^t_2$ and the central nitrogen occurred. Without a protecting group on the central nitrogen the formation of the aziridine is expected. It was decided to try and add a protecting TMS group to the central nitrogen by reacting the amino chloride with TMS-Cl (Scheme 5.4).

Scheme 5.4
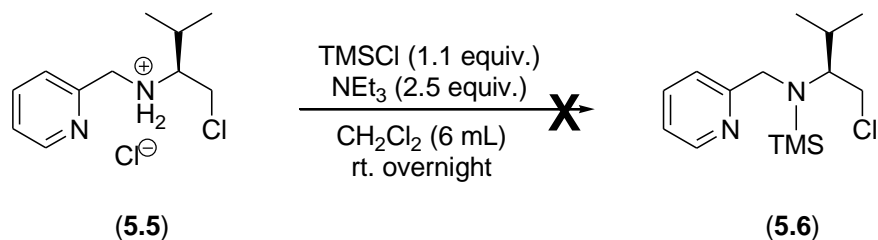
The protection reaction did not produce the desired product. Most of **5.5** remained unreacted due to limited solubility. To improve the solubility of **5.5** TMS-Cl was used as the solvent. The solubility of **5.5** improved but ^{1}H NMR analysis revealed that self-alkylation had occurred producing the aziridine. The preference towards self-alkylation can be attributed to two factors; the first is that the sterics caused by the isopropyl group would not allow addition of the TMS group and the second is that the reaction producing the aziridine is more favourable. With these two factors it was decided to react **5.5** with LiPBu$^t_2$ without the addition of the protecting group (Scheme 5.5). With the low reaction

temperature and sterics caused by the isopropyl group, a reaction between **5.5** and LiPBu$^t_2$ was expected to give **5.7**.

Scheme 5.5

| (**5.5**) | (**5.7**) |
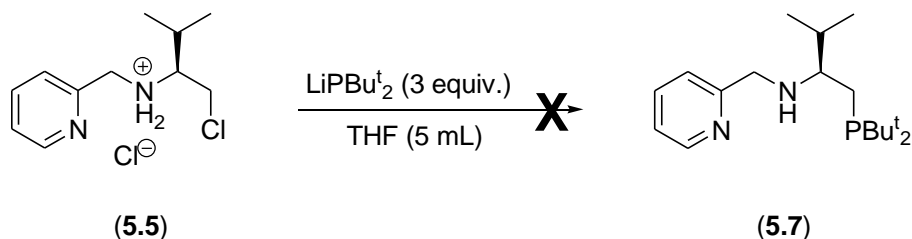
Addition of the solvent was done through vacuum transfer with the reaction mixture cooled to -80 °C. The reaction mixture was left stirring for 1 h. It was then removed from the cold bath and left stirring at room temperature for 30 min. Finally the reaction mixture was refluxed for 30 min. The purpose of the lower temperature at the beginning of the reaction was to decrease the rate of aziridine formation. To remove excess LiPBu$^t_2$ water was added to the reaction mixture. Unfortunately the ^{31}P {^{1}H} NMR spectrum showed one peak at δ 21.1 which is indicative of HPBu$^t_2$ and no peak representing the PBu$^t_2$ group of **5.7**. Analysis of the final product using ^{1}H NMR revealed no formation of **5.7** and a mixture of unreacted **5.5** and the aziridine.

Recently Babu and coworkers reported successfully using zinc powder to deprotonate an amino acid methyl ester hydrochloride salt.[47] TMSCl was then added as a protecting group during the synthesis of the peptide. Since **5.5** displays similar characteristics to the hydrochloride salt used by them, it was decided to attempt a similar synthesis using the zinc powder (Scheme 5.6).

Scheme 5.6

(**5.5**)   (**5.8**)
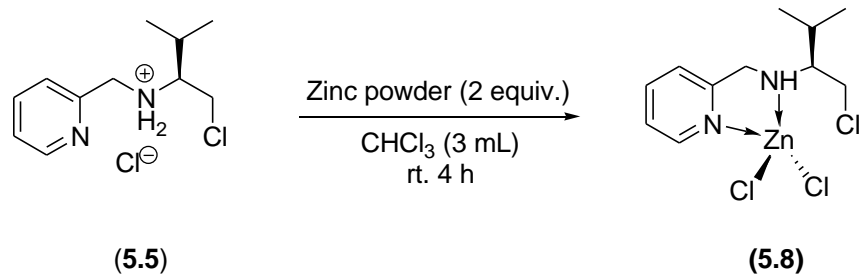
The overall yield of the final product was not determined due to the presence of unreacted zinc. The ^{1}H NMR spectrum showed the coordination of zinc to the amino chloride. The shifts of the pyridine ring were as expected. No evidence of aziridine formation was indicated by the spectrum and a multiplet at δ 3.88 represented the CH$_2$Cl group. Coordination of zinc to the amino chloride was apparent with the splitting of the NH group at δ 3.72 where the broad shift was now a multiplet. With ZnCl$_2$ acting as a protecting group on **5.8**, investigations for the addition of PBu$^t_2$ started with reacting **5.8** directly with LiPBu$^t_2$ (Scheme 5.7).

Scheme 5.7

(**5.8**)   (**5.9**)
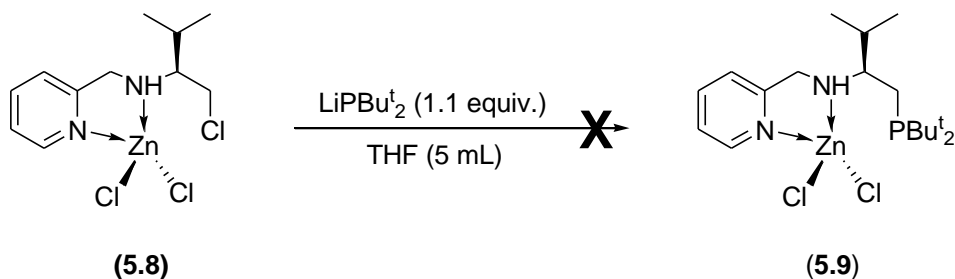
Vacuum transfer of the solvent to the reaction flask was performed. The resulting reaction mixture was left stirring for 1 h at -80 °C and 1 h at room temperature. NMR analysis showed there was no formation of **5.9**. Determining of the exact nature of **5.8** and the correct reaction scheme are still being investigated.

A final attempt for addition of the phosphine group was performed by reacting the amino alcohol (**5.4**) with ClPBu$^t_2$ (Scheme 5.8). The reaction was left heating overnight at 100 ^{o}C.

Scheme 5.8

(**5.4**)　　　　　　　　　　　　　　　　　　　　　　　(**5.7**)
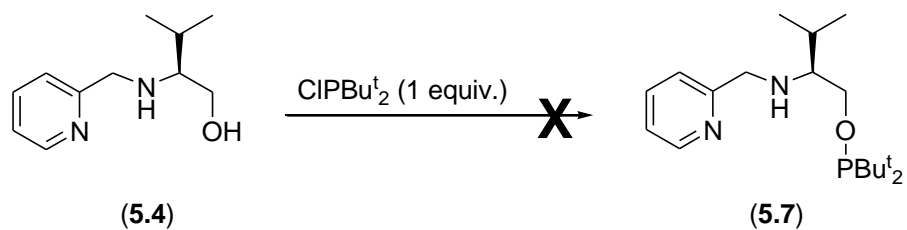
^{1}H NMR analysis of the reaction solution gave no evidence of the formation of **5.7**. The ^{31}P {^{1}H} NMR showed a peak at δ 150.6 belonging to ClPBu$^t_2$. Altering the reactions conditions also gave no evidence of **5.7**.

Chapter 6

6.1 Conclusions

In conclusion the synthesis and complete characterization of a new PNHN ligand (**2.13**) through simple organic reactions has been reported. Further studies showed the successful coordination of the PNHN ligand to iridium and ruthenium transition metals. It was discussed that the characterization and catalysis of the iridium hydrides (**3.5** and **3.6**) was hindered due to poor solubility and the inability to separate the metal complex. Successful characterization of the ruthenium dichloride (**4.4**) and dihydride (**4.7**) was achieved. Transfer hydrogenation of various ketones was then attempted using **4.7**. Some catalytic activity was observed with acetophenone and cyclohexanone at low rates. An investigation for isolation and characterization of complex **4.8** revealed a structural changed by the ligand from facial (**4.7**) to meridional (**4.8**) during catalysis. Synthesis employing RuCl$_2$(PPh$_3$)$_3$ to produce the ruthenium carbonyl complex (**4.9**) reported by Morales-Morales and coworkers was used. With the ruthenium dichloride **4.10**, synthesis of the ruthenium dihydride was attempted. Preparation of the dihydride was not achieved due to the loss to H$_2$. Further experimental investigation of the hydride ruthenium carbonyl complex is underway. With the use of the synthesis for the amino alcohol (**4.5**) by Cleij and coworkers a new chiral amino chloride (**5.5**) was produced. Studies into the addition of the phosphine group and the completion of a new chiral PNHN ligand for metal coordination are still in progress.

6.2 Future Work

With promising results from the coordination chemistry of **2.13** with ruthenium and iridium, syntheses of the new chiral PNHN ligand has become our goal. By employing L-valinol we were able to obtain the backbone structure of the desired ligand. To date the difficulty has been with the addition of the phosphine group. Alternative methods being explored for the addition of the phosphine group include exploring a ring opening reaction involving 2-isopropylaziridine (**6.1**) (Scheme 6.1).

Scheme 6.1

HN⟨ —— TMSCl / NEt$_3$, CH$_2$Cl$_2$ —→ TMS—N⟨ —— LiPBu$^t_2$ / THF —→ TMS—N(H)—...—PBu$^t_2$

(**6.1**)　　　　　　　(**6.2**)　　　　　　　(**6.3**)

—— TBAF or Et$_3$N•3HF / THF —→ H$_2$N—...—PBu$^t_2$

(**6.4**)
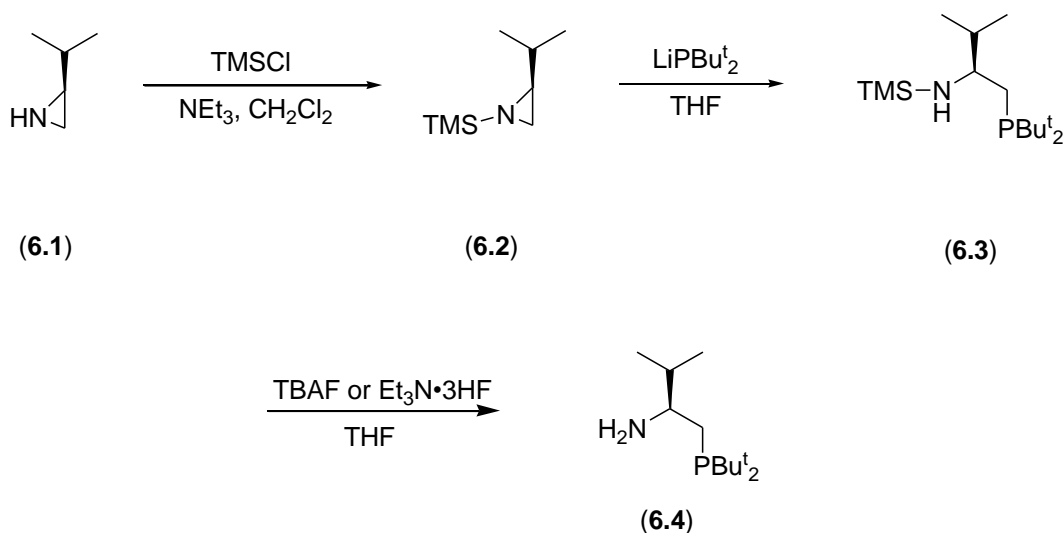
Deprotection of **6.3** would be achieved be employing TBAF or Et$_3$N•3HF depending our success toward isolation of **6.4**. Completion of the chiral PNHN ligand (**2.13**) will involve the condensation reaction between **6.4** and 2-pyridine-carboxaldehyde (**2.1**) (Scheme 6.2), followed by the reduction of the imine group employing DIBAL-H.

Scheme 6.2

(2.1) (6.4) THF rt. 1 h (2.4)

1) DIBAL-H (1.15 equiv.)
rt. 1 h
2) H$_2$O

Hexanes

(2.13)
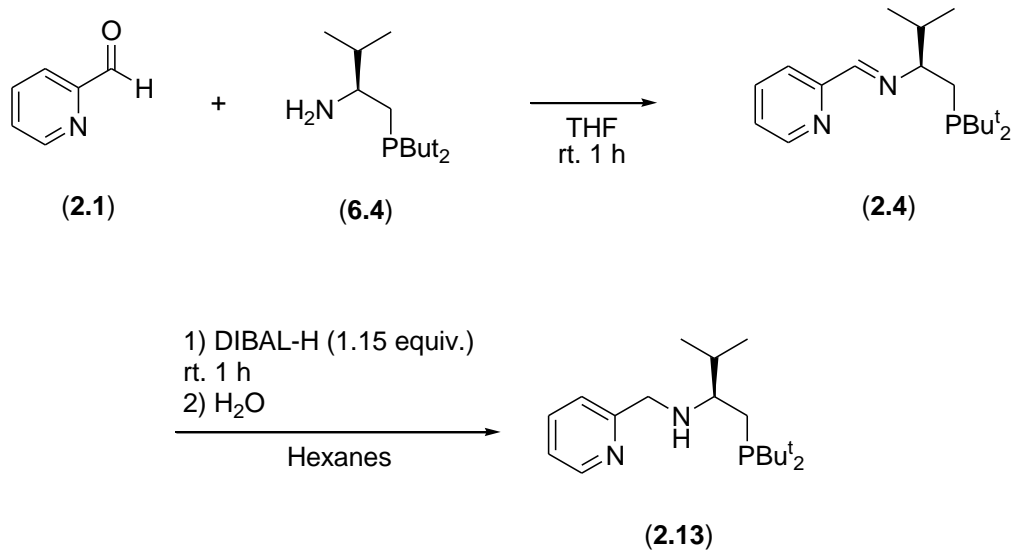
With the completion of **2.13**, coordination chemistry would involve the use of the same starting metal complexes [IrCl(COE)$_2$]$_2$, [IrCl$_3$·3H$_2$O]$_2$, [RuCl$_2$(p-cymene)]$_2$ and RuCl$_2$(PPh$_3$)$_3$. Scheme 6.3 illustrates an example of a hydride complex (**6.5**).

Scheme 6.3

(2.13) [IrCl(COE)$_2$]$_2$ (6.5)
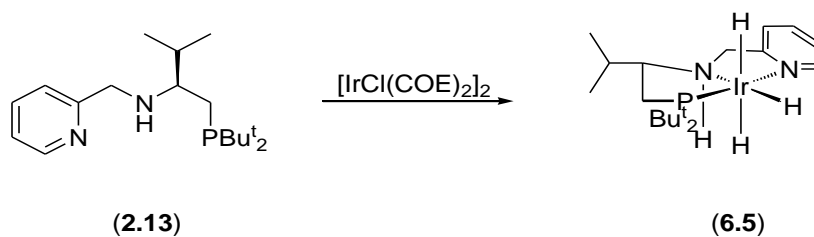
The catalytic ability of the chiral metal complex will then be analyzed by performing asymmetric hydrogenation on various ketones. The catalytic cycle is expected to follow the bifunctional mechanism depicted in Scheme 6.4.

Scheme 6.4
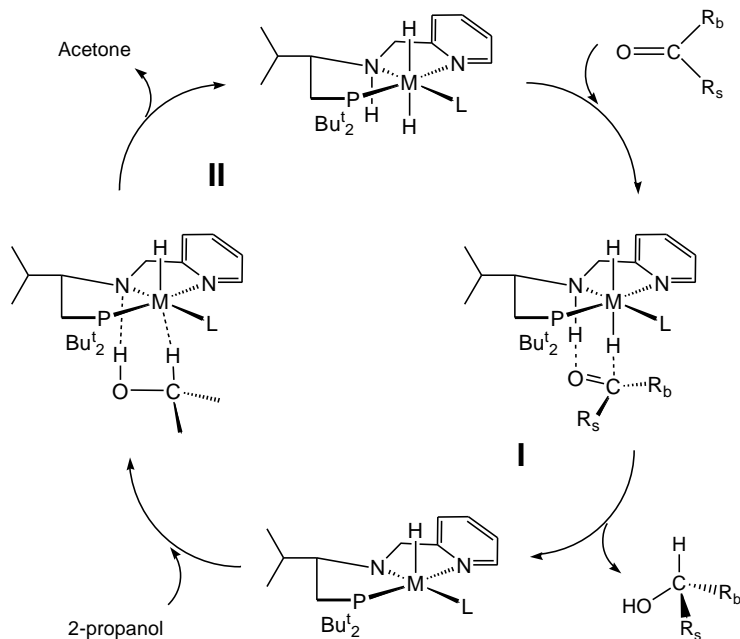
Sterics caused by the bulky Bu^t groups on the phosphine and the isopropyl group will help with the selectivity of the products. The groups R_s and R_b represent the small and bulky groups of the substrate. It is reasonable to expect that the substrate would preferably approach the catalyst with the R_b group pointing away from the bulky Bu^t groups (step **I**); therefore the final product should be mostly one enantiomer of the chiral alcohol R_sR_bCHOH. For example the hydrogenation of acetophenone is expected to give (S)-1-phenylethanol as the main product. Regeneration of the active chiral catalyst will result from transfer hydrogenation involving a molecule of 2-propanol and the unsaturated amido complex (step **II**). Finally variations of the chiral PNHN ligand will be explored using other polar and non-polar amino acids. This is because the group at the chiral center can have a range of different effects on the efficiency of the catalyst due to sterics. Amino acids of interest are *Leu* ($R = CH_2Pr^i$), *Phe* ($R = CH_2Ph$), and *Cys* ($R = CH_2SH$).

Chapter 7

7.1 Experimental Section

7.1.1 General Considerations

All preparations and manipulations were carried out under nitrogen, argon, hydrogen or carbon monoxide atmospheres with the use of gloveboxes, vacuum line and standard Schlenk flasks. Standard solvents and deuterated solvents were degassed and dried before use in reactions. Starting materials and reagents were purchased from Aldrich. NMR spectra were recorded on a Varian Unity Inova 300 MHz spectrometer. ^{1}H and ^{13}C NMR chemical shifts were measured relative to the solvent peaks. A Perkin-Elmer Spectrum BXII FT IR spectrometer was employed to obtain infrared spectra for the metal complexes.

7.1.2 Preparations

$$\text{TMS}_{\diagdown}\text{N}_{\diagup}\text{Cl}$$
$$\text{TMS}^{\diagup}$$
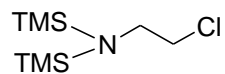
(Me$_3$Si)$_2$N(CH$_2$)$_2$Cl: A 1 L flask was charged with H$_2$N(CH$_2$)$_2$Cl•HCl (20.0 g, 172.4 mmol), triethylamine (80 mL, 568.8 mmol) and 220 mL of CH$_2$Cl$_2$. The reaction solution was cooled to 0 °C and trimethylchlorosilane (50 mL, 379.3 mmol) in 80 mL of CH$_2$Cl$_2$ was added in portions over a 5 min period to the reaction flask with vigorous stirring. The reaction mixture was stirred for 72 h. After filtration, CH$_2$Cl$_2$ was evaporated under vacuum and the product was extracted from the resulting oil with 3 x 30 mL of hexane. Hexane was evaporated under vacuum to give 24.5 g (109.5 mmol, 64 %) of (Me$_3$Si)$_2$N(CH$_2$)$_2$Cl as a clear colourless liquid. ^{1}H NMR (C$_6$D$_6$): δ 3.13 (m, 2H, C*H*$_2$Cl), 3.05 (m, 2H, NC*H*$_2$), 0.02 (s, 18H, C*H*$_3$). ^{13}C{^{1}H} NMR (C$_6$D$_6$): δ 48.09 (s, *C*H$_2$Cl), 45.39 (s, N*C*H$_2$), 2.28 (s, 18H, *C*H$_3$).

$$\text{H}_2\text{N}_{\diagup\diagdown}\text{PBu}^{\text{t}}{}_2$$
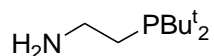
H$_2$N(CH$_2$)$_2$PBu$_2$^{t}: ClPBu$_2$^{t} (13.0 g, 71.9 mmol) was added in ca. 2 g portions to a stirred suspension of lithium granules (1.5 g, 216.0 mmol) in THF (50 mL). Each subsequent portion was added when the mixture cooled to or near room temperature. The resulting mixture was then stirred vigorously for 72 h. The mixture was then filtered and cooled to -35 °C and a solution of (Me$_3$Si)$_2$N(CH$_2$)$_2$Cl (9.0 g, 40.2 mmol) in 10 mL of THF was added dropwise over a 10 min period. The mixture was removed from the cold bath after 30 min, stirred for 3 h at room temperature and refluxing for 1 h. Water (40.0 mL) was added to the reaction flask and stirring continued for 1 h. Further washing of the solution

was done with three 5.0 mL portions of water. The resulting aqueous layer was removed

and the solvent evaporated under vacuum giving $(Me_3Si)_2N(CH_2)_2PBu_2^t$ (11.2 g, 29.3

mmol) ($^{31}P\{^1H\}$ NMR (C_6D_6): δ 27.1) contaminated with ca. 15 mol% of the dimer

$(PBu_2^t)_2$ ($^{31}P\{^1H\}$ NMR (C_6D_6): δ 40.6). Deprotection of the amino phosphine was

achieved using $Et_3N\cdot 3HF$ (3.1 g, 19.5 mmol) with triethylamine (11.8 g, 117.2 mmol) in

50 mL of CH_2Cl_2. The mixture was left stirring overnight. K_2CO_3 (4.1 g, 29.3 mmol) was

then added and the resulting heterogeneous mixture was stirred for 3 h. CH_2Cl_2 was

evaporated and 20 mL of hexane was added to the flask. The hexane solution was filtered

followed by evaporation of hexane under vacuum. $H_2N(CH_2)_2PBu_2^t$ was isolated by

distillation (b. p. = 29 – 39 °C, 0.01 mmHg) and obtained as a clear colourless liquid,

(3.7 g, 19.8 mmol, 77 %). ^1H NMR (C_6D_6): δ 3.42 (s, 2H, H_2N), 2.80 (dt, $^3J_{HH}$ = 9.0, 2H,

H_2NCH_2), 1.38 (m, 2H, CH_2P), 1.07 (d, $^3J_{HP}$ = 10.7, 18H, CH_3). $^{13}C\{^1H\}$ NMR (C_6D_6): δ

43.79 (d, $^2J_{CP}$ = 29.9, H_2NCH_2), 31.52 (d, $^1J_{CP}$ = 21.6, PC), 30.22 (d, $^2J_{CP}$ = 13.9, CH_3),

27.45 (d, $^1J_{CP}$ = 22.0, CH_2P). $^{31}P\{^1H\}$ NMR (C_6D_6): δ 20.3.
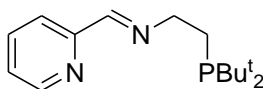
(E)-2-(di-tert-butylphosphino)-*N*-((pyridin-2-yl)methylene)ethanamine   (PNN

Ligand): To a solution of $H_2N(CH_2)_2PBu_2^t$ (3.7 g, 19.7 mmol) in 30 mL of THF, 2-

pyridine-carboxaldehyde (2.3 g, 21.7 mmol) was added dropwise over a 5 min period

with stirring. The reaction solution was left stirring for 1 h followed by evaporation of the

solvent and subsequent drying for 4 h under vacuum. The product was obtained as a clear

dark orange oil (5.3 g, 96 %). ^1H NMR (C_6D_6): δ 8.62 (s, 1H, CHN), 8.48 (m, 1H, *Py*),

8.21 (m, 1H, *Py*), 7.07 (m, 1H, *Py*), 6.64 (m, 1H, *Py*), 3.83 (m, 2H, NCH_2), 1.78 (m, 2H,

CH_2P), 1.05 (d, $^3J_{HP}$ = 10.8, 18H, CH_3). ^{13}C{^{1}H} NMR (C$_6$D$_6$): δ 162.45 (s, CHN),

156.26 (s, Py), 149.96 (s, Py), 136.32 (s, Py), 124.71 (s, Py), 121.15 (s, Py), 63.07 (d, $^2J_{CP}$

= 34.6, NCH_2), 31.66 (d, $^1J_{CP}$ = 22.1, PC), 30.09 (d, $^2J_{CP}$ = 14.0, CH$_3$), 24.11 (d, $^1J_{CP}$ =

22.8, CH_2P). ^{31}P{^{1}H} NMR (C$_6$D$_6$): δ 24.5.
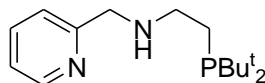
2-(di-tert-butylphosphino)-*N*-((pyridin-2yl)methyl)ethanamine (PNHN Ligand): To

a solution of the PNN Ligand (4.2 g, 15.1 mmol) in 20 mL of hexanes, DIBAL-H (2.5 g,

17.4 mmol) was added dropwise over a 10 min period with continuous stirring. The

resulting dark brownish red solution was left stirring for 1 h. The reaction solution was

then quenched with the dropwise addition of degassed water (1.6 g, 87.1 mmol) over a 10

min period with continuous stirring. The resulting orange mixture was left stirring for 30

min followed by evaporation and drying for 4 h under vacuum. The PNHN ligand was

isolated as a clear light orange oil (3.8 g, 15.1 mmol, 91 %). ^{1}H NMR (C$_6$D$_6$): δ 8.45 (d,

$^3J_{HH}$ = 4.5, 1H, Py), 7.13 (s, 1H, Py), 7.06 (m, 1H, Py), 6.59 (m, 1H, Py), 3.91 (s, 2H,

CH_2NH), 2.82 (q, $^3J_{HH}$ = 7.8, 2H, NHCH_2), 1.85 (s, 1H, NH), 1.52 (m, 2H, CH_2P), 1.02

(d, $^3J_{HP}$ = 10.8, 18H, CH_3). ^{13}C{^{1}H} NMR (C$_6$D$_6$): δ 161.78 (s, Py), 149.81 (s, Py),

136.17 (s, Py), 122.23 (s, Py), 121.91 (s, Py), 56.11 (s, CH$_2$NH), 51.07 (d, $^2J_{CP}$ = 31.2,

NHCH_2), 31.5 (d, $^1J_{CP}$ = 22.0, PC), 30.12 (d, $^2J_{CP}$ = 13.9, CH$_3$), 23.29 (d, $^1J_{CP}$ = 22.0,

CH_2P). ^{31}P{^{1}H} NMR (C$_6$D$_6$): δ 22.4.
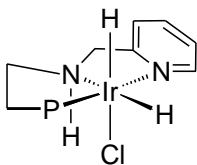
(**3.0**)

IrH₂Cl(PNHN). The PNHN ligand (180.0 mg, 0.6 mmol) was added to a solution of [IrCl(COE)₂] (280.0 mg, 0.6 mmol) in 5 ml of toluene. The reaction solution was stirred under nitrogen for 30 min. 3 freeze − pump - thaw cycles were used to refill the flask with H_2 and stirring continued for 1 h at room temperature. H_2 was then evacuated and the solution was left stirring under vacuum overnight. The mixture was filtered and washed with 3 x 2 mL of hexane and dried under vacuum for 3 h. 163 mg of IrH₂Cl(PNHN) and residual solvent was obtained as a pale green solid. IR (KBr cm⁻¹): v_{NH} = 3363 (s), v_{IrH} = 2273 (s), 2185 (s). ¹H NMR (CD₂Cl₂): δ 9.08 (d, $^3J_{HH}$ = 5.7, 1H, *Py*), 7.72 (m, 1H, *Py*), 7.26 (d, $^3J_{HH}$ = 7.8, 1H, *Py*), 7.17 (t, $^3J_{HH}$ = 6.6, 1H, *Py*), 4.81 (dd, $^3J_{HH}$ = 14.7, $^2J_{HH}$ = 4.2, 1H, PyC*H₂*), 3.99 (dd, $^3J_{HH}$ = 14.7, $^2J_{HH}$ = 10.8, 1H, PyC*H₂*), 4.37 (m, 1H, N*H*), 3.54 (m, 1H, NHC*H₂*), 2.59 (m, 1H, NHC*H₂*), 2.33 (dd, $^3J_{HH}$ = 15, $^2J_{HH}$ = 4.8, 1H, C*H₂*P), 2.06 (m, 1H, C*H₂*P), 1.32 (d, $^2J_{HP}$ = 8.1, 18H C*H₃*), -19.89 (dd, $^2J_{HP}$ = 17.7, $^2J_{HH}$ = 7.5 1H, Ir*H*), -25.28 (dd, $^2J_{HP}$ = 21.9, $^2J_{HH}$ = 7.5, 1H, Ir*H*). ³¹P {¹H} NMR (CD₂Cl₂): δ 54.0.
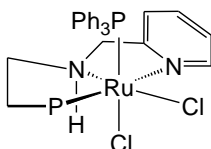
RuCl₂(PPh₃)(PNHN). A solution of RuCl₂(PPh₃)₃ (432.0 mg, 0.4 mmol) and the PNHN ligand (132.0 mg, 0.4 mmol) was stirred in 8 mL of toluene for 3 h under nitrogen at

room temperature. The resulting solid was filtered and washed with 3 x 2 mL of toluene. The solid was dried under vacuum for 3 h affording $RuCl_2(PPh_3)(PNHN)$ as light orange coloured solid (281.0 mg, 0.4 mmol, 89 %). IR (KBr cm^{-1}): ν_{NH} = 3186 (s). ^{1}H NMR (C$_6$D$_6$): δ 8.50 (m, 1H, *Py*), 8.23 (m, 6H, P*Ph$_3$*), 7.08 (m, 9H, P*Ph$_3$*), 6.64 (dt, $^3J_{HH}$ = 1.8, 7.8, 1H, *Py*), 6.36 (d, $^3J_{HH}$ = 7.5, 1H, *Py*), 6.01 (t, $^3J_{HH}$ = 6.3, 1H, *Py*), 5.78 (s, 1H, N*H*), 5.25 (t, $^3J_{HH}$ = 12.9, 1H, PyC*H$_2$*), 3.22 (m, 1H, PyC*H$_2$*), 3.06 (m, 1H, NHC*H$_2$*), 2.58 (m, 1H, NHC*H$_2$*), 1.96 (m, 2H, C*H$_2$*P), 1.26 (d, $^2J_{HP}$ = 11.7, 9H, C*H$_3$*), 1.15 (d, $^2J_{HP}$ = 11.1, 9H, C*H$_3$*). ^{31}P {^{1}H} NMR (C$_6$D$_6$): δ 52.9 (d, $^2J_{PP}$ = 21.1, 1P, Ru*P*), 40.1 (d, $^2J_{PP}$ = 21.1, 1P, Ru*P*).
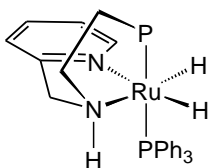
RuH$_2$(PPh$_3$)(PNHN). KOBu^t (73.0 mg, 0.6 mmol) was added to $RuCl_2(PPh_3)(PNHN)$ (221.0 mg, 0.3 mmol) dissolved in 15 mL of 2-pentanol.The solution was left stirring overnight at room temperature. The resulting dark redish brown mixture was evaporated under vacuum. A brownish orange solid (205.0 mg, 0.3 mmol) was obtained with residual 2-pentanol and KCl contaminate. IR (KBr cm^{-1}): ν_{NH} = 3308 (s), ν_{RuH} = 1909 (s, overlapped), 1888 (s, overlapped). ^{1}H NMR (THF-d$_8$): δ 8.05 (d, $^3J_{HH}$ = 5.4, 1H, *Py*), 7.56 (m, 6H, P*Ph$_3$*), 7.05 (m, 9H, P*Ph$_3$*), 7.01 (m, overlapped, 1H, *Py*), 6.69 (d, | $^3J_{HH}$ = 7.5, 1H, *Py*), 6.11 (t, $^3J_{HH}$ = 6.0, 1H, *Py*), 3.69 (m, 2H, PyC*H$_2$*), 3.41 (m, 1H, N*H*), 2.70 (m, 1H, NHC*H$_2$*), 2.60 (m, 1H, NHC*H$_2$*), 1.87 (m, 1H, C*H$_2$*P), 1.74 (m, 1H, C*H$_2$*P), 1.45 (d, $^2J_{HP}$ = 11.7, 9H, C*H$_3$*), 1.12 (d, $^2J_{HP}$ = 11.4, 9H, C*H$_3$*), -17.96 (m, 1H, Ru*H*), -18.46 (m, 1H, Ru*H*). ^{13}C {^{1}H} NMR (THF-d$_8$): δ 160.3 (d, $^3J_{CP}$ = 1.4, *C*N), 156.0 (d, $^3J_{CP}$ = 1.4,

*C*HN), 143.1 (dd, $^1J_{CP}$ = 27.9, $^3J_{CP}$ = 1.5, P*Ph₃*), 134.3 (d, J_{CP} = 11.6, P*Ph₃*), 130.3 (s, *Py*), 127.7 (d, J_{CP} = 7.8, P*Ph₃*), 127.5 (d, J_{CP} = 1.4, P*Ph₃*), 122.9 (s, *Py*), 119.0 (s, *Py*), 58.5 (s, Py*C*H₂N), 53.8 (dd, $^3J_{CP}$ = 3.9, 10.5, N*C*H₂), 38.3 (dd, $^1J_{CP}$ = 5.2, $^3J_{CP}$ = 2.7, P*C*), 31.0 (d, $^2J_{CP}$ = 7.6, *C*H₃), 24.5 (d, $^1J_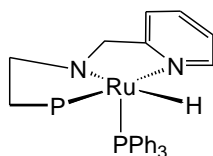{CP}$ = 14.1, *C*H₂P). ^{31}P {^{1}H} NMR (THF-d₈): δ 104.1 (d, $^2J_{PP}$ = 291.6, 1P, Ru*P*), 69.4 (d, $^2J_{PP}$ = 291.6, 1P, Ru*P*).


RuH(PPh₃)(PNN). A sample of RuH₂(PPh₃)(PNHN) (25.0 mg) in THF-d₈ was prepared in a J. Jung NMR tube. Freeze − pump − thaw cycles were repeated every 30 min with intermittent heating at 50 °C for 5 min. The resulting amido complex was obtained in solution (70 %). ^{1}H NMR (THF-d₈): δ 7.68 (m, 6H, P*Ph₃*), 7.45 (d, $^3J_{HH}$ = 5.7, 1H, *Py*), 7.24 (m, overlapped, 1H, *Py*), 7.16 (m, 9H, P*Ph₃*), 7.05 (m, overlapped, 1H *Py*), 6.18 (t, $^3J_{HH}$ = 6.3), 4.52 (m, 2H, PyC*H₂*), 3.42 (m, 1H, NC*H₂*), 3.09 (m, 1H, NC*H₂*), 2.27 (m, C*H₂*P), 2.06 (m, 1H, C*H₂*P), 1.22 (d, $^2J_{HP}$ = 11.4, 9H, C*H₃*), 0.58 (d, $^2J_{HP}$ = 11.7, 9H, C*H₃*), -19.52 (dd, $^2J_{HP}$ = 51.3, $^2J_{HP}$ = 21.9, 1H, Ru*H*). ^{13}C {^{1}H} NMR (THF-d₈): δ 170.3 (d, $^3J_{CP}$ = 1.4, *C*N), 155.8 (d, $^3J_{CP}$ = 1.4, *C*HN), 143.2 (d, J_{CP} = 29.6, P*Ph₃*), 136.2 (d, J_{CP} = 10.5, P*Ph₃*), 133.2 (s, *Py*), 128.6 (d, J_{CP} = 1.7, P*Ph₃*), 127.7 (d, J_{CP} = 8.2, P*Ph₃*), 120.3 (d, J_{CP} = 2.2, *Py*), 119.2 (s, *Py*), 43.0 (s, broad, *C*H₂N), 37.9 (m, P*C*) 34.9 (m, P*C*), 30.4 (d, $^2J_{CP}$ = 5.5, *C*H₃), 30.0 (d, $^2J_{CP}$ = 5.1, *C*H₃), 20.0 (s, N*C*H₂), 14.7 (s, *C*H₂P). ^{31}P {^{1}H} NMR (THF-d₈): δ 109.8 (d, $^2J_{PP}$ = 16.5, Ru*P*), 73.8 (d, $^2J_{PP}$ = 16.6, Ru*P*).
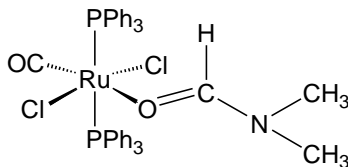
RuCl$_2$(CO)(PPh$_3$)$_2$(dmf).[46] A mixture of RuCl$_2$(PPh$_3$)$_3$ (2.0 g, 2.1 mmol) in 15 mL of dmf was stirred for 1 h under carbon monoxide at room temperature. The resulting pale yellow suspension was filtered and washed with 3 x 15 mL of ether. Subsequent drying under vacuum for 3 h afforded RuCl$_2$(CO)(PPh$_3$)$_2$(dmf) as a pale yellow solid (1.4 g, 2.1 mmol, 83 %). IR (KBr cm^{-1}): ν_{CO} = 1913 (s), ν_{CN} = 1631 (vs). ^{1}H NMR (CD$_2$Cl$_2$): δ 7.72 (m, 12H, P*Ph$_3$*), 7.38 (m, 18H, P*Ph$_3$*), 6.81 (s, 1H, C*H*(DMF)), 2.26 (s, 3H, C*H$_3$*(DMF)), 2.20 (s, 3H, C*H$_3$*(DMF)). ^{31}P {^{1}H} NMR (CD$_2$Cl$_2$): δ 35.9 (s, 2P, Ru*P*).
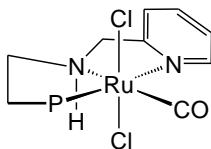
RuCl$_2$(CO)(PNHN). PNHN (384.0 mg, 1.4 mmol) was added to RuCl$_2$(CO)(PPh$_3$)(dmf) (994.0 mg, 1.2 mmol) dissolved in 15 mL of glyme. The solution was left stirring at 90 °C for 4 h. The resulting mixture was then cooled to room temperature and left stirring overnight. The solid material was filtered and washed with 3 x 2 mL of ether. The solid was then dried for 4 h affording RuCl$_2$(CO)(PNHN) as a yellow solid (464.0 mg, 1.2 mmol, 88 %). IR (KBr cm^{-1}): ν_{NH} = 3178 (s), ν_{CO} = 1929 (s), ν_{CN} = 1607 (vs). ^{1}H NMR (CD$_2$Cl$_2$): δ 8.94 (m, 1H, *Py*), 7.73 (m, 1H, *Py*), 7.32 (m, overlapped, 1H, *Py*), 7.29 (m, overlapped, 1H, *Py*), 5.16 (m, 1H, N*H*), 4.87 (m, 1H, PyC*H$_2$*), 4.51 (m, 1H, PyC*H$_2$*), 3.67 (m, 1H, NHC*H$_2$*), 3.37 (m, overlapped, 1H, NHC*H$_2$*), 2.52 (m, 1H, C*H$_2$*P), 2.24 (m, 1H, C*H$_2$*P), 1.45 (d, ^3J = 12.9, 9H, C*H$_3$*), 1.38 (d, ^3J = 12.9, 9H, C*H$_3$*). ^{13}C {^{1}H} NMR

(CD$_2$Cl$_2$): δ 203.8 (d, ^2J = 14.2, *C*O), 161.6 (s, *C*N), 153.9 (s, *C*H), 137.8 (s, *C*H), 124.9

(d, $^3J_{CP}$ = 2.1, *C*H), 122.1 (d, $^4J_{CP}$ = 1.8, *C*H), 57.4 (s, *C*H$_2$NH), 50.1 (s, NH*C*H$_2$), 39.6 (t,

$^1J_{CP}$ = 17.7, P*C*CH$_3$), 31.2 (t, ^2J = 3.1, *C*H$_3$), 28.0 (d, ^1J = 15.3, *C*H$_2$P). ^{13}P {^{1}H} NMR

(CD$_2$Cl$_2$): δ 86.5.
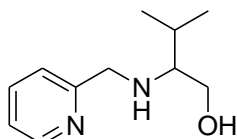
3-methyl-2-(pyridin-2-ylmethylamino)butan-1-ol (5.4). [47] A 300 mL flask was charged

with L-valinol (5.0 g, 48.4 mmol), 5 g of molecular sieves and 50 mL of CH$_2$Cl$_2$. A

solution of 2-pyridine-carboxaldehyde (5.3 g, 49.9 mmol) and 50 mL of CH$_2$Cl$_2$ was

added dropwise to the reaction flask over 10 min. with continuous stirring. The reaction

solution was left stirring for 3 h under an open line with a continuous flow of argon. The

solid precipitate was filtered off and CH$_2$Cl$_2$ was evaporated under vacuum. 100 mL of

dry ethanol was added to the resulting clear colourless oil. The reaction flask was cooled

in an ice bath and a suspension of NaBH$_4$ (7.3 g, 193.9 mmol) in 50 mL of dry ethanol

was added with continuous stirring. The reaction solution was left stirring at room

temperature, under argon, overnight. Ethanol was then evaporated and the crude product

was treated with 50 mL of 10 % aqueous Na$_2$CO$_3$ and stirred for 1 h. The product was

extracted with 3 x 70 mL of CHCl$_3$. The solvent was evaporated and the resulting oil

dried under vacuum for 3 h. The product was obtained as a clear pale yellow oil (8.8 g,

48.4 mmol, 94 %). ^{1}H NMR (CHCl$_3$): δ 8.51 (m, 1H, *Py*), 7.62 (m, 1H, *Py*), 7.25 (m,

overlapped, 1H, *Py*), 7.14 (m, 1H, *Py*), 3.97 (dd, $^2J_{HH}$ = 14.7, 2H, Py*CH$_2$*), 3.65 (dd, $^2J_{HH}$

= 12.0, 1H, C*H$_2$*OH), 3.45 (dd, $^2J_{HH}$ = 12.0, 1H, C*H$_2$*OH), 3.36 (s, 1H, N*H*), 2.47 (m, 1H,

NHC*H*), 1.82 (m, 1H, C*H*(CH$_3$)$_2$), 0.96 (d, $^3J_{HH}$ = 6.9, 3H, C*H*$_3$), 0.90 (d, $^3J_{HH}$ = 6.9, 3H, C*H*$_3$). ^{13}C {^{1}H} NMR (CHCl$_3$): δ 160.2 (s, *C*N), 149.2 (s, *Py*), 136.8 (s, *Py*), 122.4 (s, *Py*), 122.2 (s, *Py*), 65.0 (s, NH*C*H), 61.5 (s, *C*H$_2$OH), 52.6 (s, *C*H$_2$NH), 29.7 (s, *C*H(CH$_3$)$_2$), 19.7 (s, *C*H$_3$), 18.9 (s, *C*H$_3$).
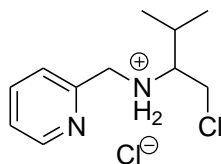
1-chloro-3-methyl-*N*-(pyridine-2-ylmethyl)butan-2-amine (5.5). A 100 mL flask was charged with **5.4** (2.0 g, 10.3 mmol) and 10 mL of CHCl$_3$. The reaction solution was cooled in an ice bath and SOCl$_2$ (0.8 mL, 10.8 mmol) was added dropwise over 30 min. with vigorous stirring. The reaction solution was left stirring in the ice bath for 10 min. then refluxed for 1 h at 40 °C. The reaction solution was then placed in the freezer for 2 h. The resulting solid was filtered, washed with CH$_2$Cl$_2$ and dried under vacuum for 2 h. The product was obtained as a beige solid (1.1 g, 10.3 mmol, 42 %). ^{1}H NMR (DMSO): δ 9.98 (s, 1H, N*H*$_2$), 8.74 (d, $^3J_{HH}$ = 4.8, 1H, *Py*), 8.14 (m, 1H, *Py*), 7.98 (d, $^3J_{HH}$ = 7.8, 1H, *Py*), 7.65 (t, $^3J_{HH}$ = 6.0, 1H, *Py*), 4.57 (s, 2H, CC*H*$_2$), 4.10 (m, 2H, C*H*$_2$Cl), 3.41 (m, 1H, NHC*H*), 2.30 (m, 1H, C*H*(CH$_3$)$_2$), 1.04 (d, $^3J_{HH}$ = 6.9, 3H, C*H*$_3$), 0.99 (d, $^3J_{HH}$ = 6.9, 3H, C*H*$_3$). ^{13}C {^{1}H} NMR (DMSO): δ 150.8 (s, *C*N), 147.3 (s, *Py*), 140.8 (s, *Py*), 126.3 (s, *Py*), 125.5 (s, *Py*), 63.4 (s, NH*C*H), 47.9 (*C*H$_2$NH), 41.4 (s, *C*H$_2$Cl), 28.1 (s, *C*H(CH$_3$)$_2$), 18.6 (s, *C*H$_3$), 17.3 (s, *C*H$_3$).
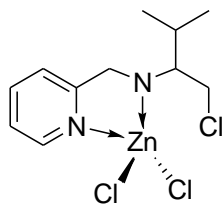
ZnCl$_2$(PyCH$_2$NHCH(CH(CH$_3$)$_2$)Cl. A 25 mL flask was first charged with **5.5** (200.0 mg, 0.7 mmol), Zn powder (92.0 mg, 1.4 mmol) and 3 mL of CHCl$_3$. The reaction mixture was stirred at room temperature for 4 h. The solvent was evaporated and the solid dried under vacuum for 4 h. The resulting product was obtained with unreacted Zn powder. ^{1}H NMR (CHCl$_3$): δ 8.60 (d, $^3J_{HH}$ = 5.1, 1H *C*N), 7.99 (m, 1H *Py*), 7.55 (t, $^3J_{HH}$ = 7.5, 1H, *Py*), 7.47 (d, $^3J_{HH}$ = 8.1, 1H, *Py*), 4.34 (m, 2H, CC*H$_2$*), 3.88 (m, 2H, C*H$_2$*Cl), 3.72 (m, 1H, N*H*), 3.28 (m, 1H, NHC*H*), 2.42 (m, 1H, C*H*(CH$_3$)$_2$), 1.12 (d, $^3J_{HH}$ = 6.9, 3H, C*H$_3$*), 1.07 (d, $^3J_{HH}$ = 6.9, 3H, C*H$_3$*).

References

[1] de Vries, J. D.; Elsevier, C. J. *The Handbook of Homogeneous Hydrogenation*, **2007**, 1-3.

[2] Samec, J. S. M.; Bäckvall, J. E.; Anderson, P. G.; Brandt, P. *Chem. Soc. Rev.* **2006**, 35, 237.

[3] Meerwein, H.; Schmidt, R. *Ann.* **1925**, 444, 221.

[4] Ponndorf, W. *Angew. Chem.* **1926**, 39, 138.

[5] Verley, A. *Bull. Soc. Chim.* **1925**, 37, 537.

[6] (a) Ohkuma, T.; Ooka, H.; Ikariya, T.; Noyori, R. *J. Am. Chem. Soc.* **1995**, 117, 10417. (b) Mikami, K.; Korenaga, T.; Terada, M.; Ohkuma, T.; Pham, T.; Noyori, R. *Angew. Chem., Int. Ed.* **1999**, 38, 495.

[7] Abdur-Rashid, K.; Lough, A. J.; Morris, R. H. *Organometallics* **2000**, 19, 2655.

[8] Johnson, N. B.; Lennon, I. C.; Moran, P. H.; Ramsden, J. A. *Acc. Chem. Res.* **2007**, 40, 1291.

[9] Ikariya, T.; Murata, K.; Noyori, R. *Org. Biomol. Chem.* **2006**, 4, 393.

[10] (a) Knowles, W. S.; Sabacky, M. J. *J. Chem. Commun.* **1968**, 1445. (b) Horner, L.; Siegel, H.; Buthe, H. *Angew. Chem., Int. Ed.* **1968**, 7, 942.

[11] (a) Shvo, Y.; Czarkie, D; Rahamim, Y.; Chodosh, D. F. *J. Am. Chem. Soc.* **1986**, 108, 7400. (b) Blum, Y.; Czarkie, D.; Rahamim, Y.; Shvo, Y. *Organometallics* **1985**, 4, 1459.

[12] Doucet, H.; Ohkuma, T.; Murata K.; Yokozawa, T.; Kozawa, M.; Katayama, E.; England, A. F.; Ikariya, T.; Noyori, R. *Angew. Chem.* **1998**, 110, 1792.

[13] Takehara, J.; Hashiguchi, S.; Fujii, A.; Inoue, S.; Ikariya, T.; Noyori, R. *Chem. Commun.* **1996**, 233.

[14] Mizushima, E.; Yamaguchi, M.; Yamagishi, T. *J. Mol. Catal. A: Chem.* **1999**, 148, 69.

[15] Lin, Y.; Zhou, Y. *Organometallics* **1990**, 381, 135.

[16] Pämies, O.; Bäckvall, J. E. *Chem. Eur. J*. **2001**, 7, 5052.

[17] Lundgren, R. J.; Rankin, M. A.; McDonald, R.; Schatte, G.; Stradiotto, M. *Angew. Chem. Int. Ed*. **2007**, 46, 4732.

[18] Noyori, R.; Yamakawa, M.; Hashiguchi, S. *J. Org. Chem*. **2001**, 66, 7931.

[19] Handgraaf, J.; Meijer, E. J. *J. Am. Chem. Soc*. **2007**, 129, 3099.

[20] Noyori, R.; Hasiguchi, S. *Acc. Chem. Res*. **1997**, 30, 97.

[21] Bi, S.; Xie, Q.; Zhao, X.; Zhao, Y.; Kong, X. *Organometallics*. **2007**, 11, 43.

[22] Clapham, S. E.; Hadzovic, A.; Morris, R. H. *Coord. Chem. Rev*. **2004**, 248, 2201.

[23] Menashe, N.; Salant, E.; Shvo, Y. *J. Organomet. Chem*. **1996**, 97, 514.

[24] Samec, J. S. M.; Bäckvall, J. E. *Chem. Eur. J*. **2002**, 8, 2955.

[25] Shvo, Y.; Goldberg, I.; Czierke, D.; Reshef, D.; Stein, Z. *Organometallics* **1997**, 16, 133.

[26] Csjernyk, G.; Éll, A. H.; Fadini, L.; Pugin, B.; Bäckvall, J. E. *J. Org. Chem*. **2003**, 68, 7681.

[27] Samec, J. S. M.; Éll, A. H.; Bäckvall, J. E. *Chem. Eur. J*. **2005**, 11, 2327.

[28] Casey, C. P.; Singer, S. W.; Powell, D. R.; Hayashi, R. K.; Kavana, M. *J. Am. Chem. Soc*. **2001**, 123, 1090.

[29] Johnson, J. B.; Bäckvall, J. *J. Org. Chem*. **2003**, 68, 7681.

[30] Baratta, W.; Chelucci, G.; Gladiali, S.; Siega, K.; Toniutti, M.; Zanette M.; Zangrando, E.; Rigo, P. *Angew. Chem. Int. Ed*. **2005**, 44, 6214.

[31] Ohkuma, T.; Koizumi, M.; Doucet, H.; Pham, T.; Kozawa, M.; Murata, K.; Katayama, E.; Yokozawa, T.; Ikariya, T.; Noyori, R. *J. Am. Chem. Soc.* **1998**, 120, 13 529.

[32] de Araujo, M. P.; de Figueiredo, A. T.; Bogado, A. L.; von Poelhsitz, G.; Ellena, J.; Castellano, E. E.; Donnici, C. L.; Comasseto, J. V.; Batista, A. A. *Organometallics*. **2005**, 24, 6159.

[33] Braunstein, P.; Fryzuk, M. D.; Naud, F.; Rettig, S. J. *J. Chem. Soc., Dalton Trans*. **1999**, 589.

[34] Braunstein, P; Naud, F.; Pfaltz, A.; Rettig, S. J. *Organometallics* **2000**, 19, 2676.

[35] Gao, J. X.; Zhang, H.; Yi, X. D.; Xu, P.P.; Tang, C. L.; Wan, H. L.; Tsai, K. R.; Ikariya, T. *Chirality* **2000**, 12, 383.

[36] Baratta, W.; Schütz, J.; Herdtweck, E.; Herrmann, W. A.; Rigo, P. *J. Organomet. Chem*. **2005**, 690, 5570.

[37] Del Zotto, A.; Baratta, W.; Ballico, M.; Herdtweck, E.; Rigo, P. *Organometallics* **2007**, 26, 5636.

[38] Guo, R.; Morris, R. H.; Song, D. *J. Am. Chem. Soc*. **2005**, 127, 516.

[39] Gagliardo, M.; Chase, P. A.; Brouwer, S.; van Klink, G. P. M.; van Koten, G. *Organometallic* **2007**, 26, 2219.

[40] Gusev, D. G.; Stradiotto, M. *Computational Research on Inner-Sphere Catalytic Transfer Hydrogenation (Presentation)*. **January 7-11 2007**, Spain.

[41] Lee, J.; Lee, Y.; Jeong, H.; Lee, J. S.; Lee, C.; Ko, J.; Kang, S. O. *Organometallics* **2003**, 22, 445.

[42] Cox, D. P.; Terpinski, J.; Lawrynowicz, W. *J. Org. Chem*. **1984**, 49, 3216.

[43] Choualeb, A.; Lough, A. J.; Gusev, D. G. *Organometallics* **2007**, 26, 5224.

[44] James, B. R.; Markham, L. D.; Hui, B. C.; Rempel, G. L. *J. Chem. Soc*. **1973**, 2247.

[45] Gómez-Benítez, V.; Olvera-Mancilla, J.; Hernández-Ortega, S.; Morales-Morales, D. *J. Mol. Struct.* **2004**, 689, 137.

[46] Cleij, M. C.; Scrimin, P.; Tecilla, P.; Tonellato, U. *Langmuir* **1996**, 12, 2956.

[47] Babu, V. V. S.; Vasanthakumar, G.; Tantry, S. J. *Tetrahedron Lett*. **2005**, 46, 4099.